RESEARCH REPORT

HEALTH EFFECTS INSTITUTE

Number 121
September 2004

Field Evaluation of Nanofilm Detectors for Measuring Acidic Particles in Indoor and Outdoor Air

Beverly S Cohen, Maire SA Heikkinen, Yair Hazi, Hai Gao, Paul Peters, and Morton Lippmann

HEALTH
EFFECTS
INSTITUTE

The Health Effects Institute was chartered in 1980 as an independent and unbiased research organization to provide high quality, impartial, and relevant science on the health effects of emissions from motor vehicles, fuels, and other environmental sources. All results are provided to industry and government sponsors, other key decisionmakers, the scientific community, and the public. HEI funds research on all major pollutants, including air toxics, diesel exhaust, nitrogen oxides, ozone, and particulate matter. The Institute periodically engages in special review and evaluation of key questions in science that are highly relevant to the regulatory process. To date, HEI has supported more than 220 projects at institutions in North America, Europe, and Asia and has published over 160 Research Reports and Special Reports.

Typically, HEI receives half of its core funds from the US Environmental Protection Agency and half from 28 worldwide manufacturers and marketers of motor vehicles and engines who do business in the United States. Other public and private organizations periodically support special projects or certain research programs. Regardless of funding sources, HEI exercises complete autonomy in setting its research priorities and in reaching its conclusions.

An independent Board of Directors governs HEI. The Institute's Health Research Committee develops HEI's five-year Strategic Plan and initiates and oversees HEI-funded research. The Health Review Committee independently reviews all HEI research and provides a Commentary on the work's scientific quality and regulatory relevance. Both Committees draw distinguished scientists who are independent of sponsors and bring wide-ranging multidisciplinary expertise.

The results of each project and its Commentary are communicated widely through HEI's home page, Annual Conference, publications, and presentations to professional societies, legislative bodies, and public agencies.

HEI STATEMENT
Synopsis of Research Report 121

Evaluation of Iron Nanofilm Detectors for Measuring Acidic Particles in Indoor and Outdoor Air

Over the last several decades, evidence has accumulated suggesting that exposure to airborne particulate matter (PM), which includes particles of varying composition and sizes (coarse, fine, and ultrafine), may affect the human cardiovascular and respiratory systems. Although ultrafine particles constitute a small percentage of the total PM mass in the size category regulated by the EPA through the National Ambient Air Quality Standards (PM < 2.5 μm in aerodynamic diameter), they are present in high number concentrations.

Much research has been conducted to learn how each component of PM contributes to its health effects in order to help inform decisions on ambient PM standards and pollution control strategies. Such research, especially in population studies, has been hampered by the lack of portable instruments that can measure the personal exposure levels of specific PM components. In 1998, HEI issued RFA 98-1, "Characterization of Exposure to and Health Effects of Particulate Matter," seeking studies to improve characterization of personal exposure to PM and to evaluate attributes of particles that may cause toxicity. In response to this RFA, Dr Beverly Cohen and colleagues at New York University Medical Center proposed to test a new iron-coated nanofilm for collecting and measuring ambient concentrations of acidic ultrafine PM. Cohen and colleagues hypothesized that because small particles are more likely than larger particles to deposit in the lower respiratory tract, and particle acidity is known to damage lung tissues, acidic ultrafine particles may be especially toxic. Until this study, none of the existing sampling methods could provide a measure of these particles.

APPROACH

The iron nanofilm detector is a thin iron-coated silicon chip (5 mm × 5 mm × 0.6 mm). The investigators assumed that, upon impact, each acidic particle would react with the iron, creating an elevated site, or bump, on the film surface. They visualized the reaction sites by scanning the surface of the film using an atomic force microscope. As shown in this report and in previous work by Cohen and colleagues, laboratory-generated acidic particles generally form reaction sites surrounded by a ring. Therefore, elevated sites with rings on iron nanofilms exposed to ambient aerosol were assumed to reflect acidic particles. Sites without rings were assumed to represent nonacidic particles. Particle number concentration was calculated from the number of impact sites counted on the scanned areas with corrections to account for the collection efficiency and other parameters specific to each sampler.

The authors tested the performance of iron nanofilms preexposed to laboratory-generated sulfuric acid particles of different sizes under a variety of storage conditions (temperature and humidity). They used two types of air samplers for ambient monitoring. One was a combined system in which an electrostatic aerosol sampler (EAS) was preceded by a microorifice impactor (MOI) that removed particles larger than 100 nm from the air samples. The other was an ultrafine diffusion monitor (UDM), which did not have specific size selectivity. Field monitoring sessions (lasting 1 or 2 weeks) were conducted during each of the four seasons in a rural area (Tuxedo NY) between July 1999 and May 2000 and during the winter of 2000 in an urban area (New York City). For these tests, the MOI-EAS and the UDM were collocated. The UDM was also deployed in two indoor environments.

Cohen and colleagues made a number of comparisons of the data obtained. They compared the number concentrations of acidic particles and of total ultrafine particles between the MOI-EAS and the UDM; the number of acidic ultrafine particles

This Statement, prepared by the Health Effects Institute, summarizes a research project funded by HEI and conducted by Dr Beverly Cohen at New York University School of Medicine, Tuxedo NY. The following Research Report contains both the detailed Investigators' Report and a Critique on the study prepared by the Institute's Health Review Committee.

measured using MOI-EAS with the acid content of particles of comparable size collected on MOI filters; and the total ultrafine particle concentrations (of acidic and nonacidic particles) determined using the MOI-EAS and the UDM with those determined using a commercially available particle counter, the scanning mobility particle sizer (SMPS).

RESULTS AND INTERPRETATION

Laboratory experiments showed that the surfaces of both blank nanofilms and nanofilms preexposed to sulfuric acid particles were generally stable for a period of 3 months, at average ambient temperature (22°C) and high humidity (92%), and were not affected substantially by exposure to particle-free ambient air. However, the surface appeared to deteriorate at high temperature (39°C, 88% humidity). Both ambient-temperature and high-temperature storage may have caused enlargement of some reaction sites, but the fact that the same areas of the detectors were not reexamined over time made it difficult to evaluate the temporal changes on the nanofilms.

The results of the monitoring studies showed limited agreement between the MOI-EAS and UDM measurements. There was no trend in the relation of acidic particle numbers measured by the two instruments. For the total particle number concentrations, however, the MOI-EAS consistently yielded lower values than those obtained with the UDM. The poor agreement between the two types of samplers can be attributed to differences in their size selectivity and efficiency of collection (with the UDM having a much lower efficiency than the EAS). In addition, the magnitude of error in the determination of deposition efficiency is not known.

The number concentrations obtained from the MOI-EAS nanofilms were lower than those derived from the comparison instrument, the SMPS, while those obtained from the UDM nanofilms were more similar to the corresponding SMPS measures for some sampling periods. Results of indoor measurements using the UDM were not compared with SMPS measurements.

The authors found no correlation between the number concentrations of acidic ultrafine particles (determined with the MOI-EAS) and the acid content of ultrafine particles (determined by measuring the pH of particles less than 100 nm in diameter collected on a filter placed in parallel with the EAS after the last stage of the MOI). This finding is intriguing and, if confirmed by further testing, suggests that conclusions about the association between health effects and exposure to acidic particles might be different if the number of acidic particles, rather than particle acidity, were evaluated.

Although the iron nanofilm is promising for acidic particle analysis, uncertainties remain to be better understood: the rate of the reaction of acidic and nonacidic particles with the nanofilm, the relation between particle acidity and the shape of the reaction site, the collection efficiency of the samplers (especially the UDM), and the error in counting the reaction sites.

Finally, it would be useful to evaluate how the nanofilms perform in locations with higher levels of particles and gases (especially ozone, which is the gas most likely to react chemically with the iron nanofilm). In the absence of other methods for measuring the number of acidic particles, iron nanofilms housed in an EAS may be used to approximate the ambient levels of acidic particles, although further improvements of the system are needed.

Library of Congress Catalog Number for the HEI Report Series: WA 754 R432.
The paper in this publication meets the minimum standard requirements of the ANSI Standard Z39.48-1984 (Permanence of Paper) effective with Report 21 in December 1988; and effective with Report 92 in 1999 the paper is recycled from at least 30% postconsumer waste with Reports 25, 26, 32, 51, 65 Parts IV, VIII, and IX, 91, 105, and 117 excepted. These excepted Reports are printed on acid-free coated paper.

CONTENTS

Research Report 121

HEALTH EFFECTS INSTITUTE

Field Evaluation of Nanofilm Detectors for Measuring Acidic Particles in Indoor and Outdoor Air

Beverly S Cohen, Maire SA Heikkinen, Yair Hazi, Hai Gao, Paul Peters, and Morton Lippmann

Department of Environmental Medicine, New York University School of Medicine, Tuxedo, New York; Division of Environmental Health Sciences, Mailman School of Public Health, Columbia University, New York, New York; and Research Center for Urban Environment, Hong Kong Polytechnical University, Hong Kong, China

HEI STATEMENT

This Statement is a nontechnical summary of the Investigators' Report and the Health Review Committee's Critique.

INVESTIGATORS' REPORT

When an HEI-funded study is completed, the investigators submit a final report. The Investigators' Report is first examined by three ouside technical reviewers and a biostatistician. The report and the reviewers' comments are then evaluated by members of the HEI Health Review Committee, who had no role in selecting or managing the project. During the review process, the investigators have an opportunity to exchange comments with the Review Committee and, if necessary, revise the report.

CRITIQUE Health Review Committee

The Critique about the Investigators' Report is prepared by the HEI Health Review Committee and staff. Its purpose is to place the studies into a broader scientific context, to point out strengths and limitations, and to discuss remaining uncertainties and implications of the findings for public health.

Continued

RELATED HEI PUBLICATIONS

Publishing History: This document was posted as a preprint on *www.healtheffects.org* and then finalized for print.

Citation for whole document:

Cohen BS, Heikkinen MSA, Hazi Y, Gao H, Peters P, Lippmann M. September 2004. Field Evaluation of Nanofilm Detectors for Measuring Acidic Particles in Indoor and Outdoor Air. Research Report 121. Health Effects Institute, Boston MA.

When specifying a section of this report, cite it as a chapter of the whole document.

INVESTIGATORS' REPORT

Field Evaluation of Nanofilm Detectors for Measuring Acidic Particles in Indoor and Outdoor Air

Beverly S Cohen, Maire SA Heikkinen, Yair Hazi, Hai Gao, Paul Peters, and Morton Lippmann

ABSTRACT

This field evaluation study was conducted to assess new technology designed to measure number concentrations of strongly acidic ultrafine particles. Interest in these particles derives from their potential to cause adverse health effects. Current methods for counting and sizing airborne ultrafine particles cannot isolate those particles that are acidic. We hypothesized that the size-resolved number concentration of such particles to which people are exposed could be measured by newly developed iron nanofilm detectors on which sulfuric acid (H_2SO_4*) droplets produce distinctive ringed reaction sites visible by atomic force microscopy (AFM). We carried out field measurements using an array of samplers, with and without the iron nanofilm detectors, that allowed indirect comparison of particle number concentrations and size-resolved measures of acidity.

The iron nanofilm detectors are silicon chips (5 mm × 5 mm × 0.6 mm) that are coated with iron by vapor deposition. The iron layer was 21.5 or 26 nm thick for the two batches used in these experiments. After exposure the detector surface was scanned topographically by AFM to view and enumerate the ringed acid reaction sites and deposited nonacidic particles. The number of reaction sites and particles per scan can be counted directly on the image displayed by AFM. Sizes can also be measured, but for this research we did not size particles collected in the field.

The integrity of the surface of iron nanofilm detectors was monitored by laboratory analysis and by deploying blank detectors and detectors that had previously been exposed to H_2SO_4 calibration aerosols. The work established that the detectors could be used with confidence in temperate climates. Under extreme high humidity and high temperature, the surface film was liable to detach from the support, but remaining portions of the film still produced reliable data. Exposure to ambient gases in a filtered air canister during the field tests did not affect the film quality.

Sampling sessions to obtain particle measurements were scheduled for two 1-week periods in each of the four seasons at a rural site in Tuxedo, New York. This schedule was selected to test outdoor performance of the iron nanofilm detectors under a variety of weather conditions. To seek possible artifacts caused by local source differences, we also sampled outdoors for two 1-week sessions during the winter in New York City. Indoor tests were conducted in the cafeteria at the Nelson Institute of Environmental Medicine (NIEM) in Tuxedo and in a residence in Newburgh, New York.

For the outdoor tests we simultaneously deployed several particle samplers to obtain several measures:

- the number concentration of acidic and total particles that penetrated the 100-nm cut size of a microorifice impactor (MOI) and were electrically precipitated in an electrostatic aerosol sampler (EAS) onto the iron nanofilm detectors;
- the number concentrations of acidic and total particles estimated from detectors placed in a simple ultrafine diffusion monitor (UDM);
- the size-fractionated mass concentration of strong acids in samples from the submicrometer collection stages of the MOI and from a polycarbonate filter, parallel to the EAS, that also collected particles penetrating the MOI's 100-nm cut size; and

* A list of abbreviations and other terms appears at the end of the Investigators' Report.

This Investigators' Report is one part of Health Effects Institute Research Report 121, which also includes a Critique by the Health Review Committee and an HEI Statement about the research project. Correspondence concerning the Investigators' Report may be addressed to Dr Beverly S Cohen, New York University School of Medicine, Department of Environmental Medicine, 57 Old Forge Road, Tuxedo NY 10987.

Although this document was produced with partial funding by the United States Environmental Protection Agency under Assistance Award R82811201 to the Health Effects Institute, it has not been subjected to the Agency's peer and administrative review and therefore may not necessarily reflect the views of the Agency, and no official endorsement by it should be inferred. The contents of this document also have not been reviewed by private party institutions, including those that support the Health Effects Institute; therefore, it may not reflect the views or policies of these parties, and no endorsement by them should be inferred.

- the number concentration of all ambient particles with diameters of 300 nm or smaller, determined using a scanning mobility particle sizer (SMPS).

In the results from these samplers, the mean number concentration of acidic particles ranged from about 100 to 1800/cm^3, representing 10% to 88% of all ambient ultrafine particles for the different seasons and sites. The number concentration did not correlate with the acidic mass (hydrogen ion, or H^+, content) for particles smaller than 100 nm in diameter. This was not surprising because a single 100-nm particle may contain the same acid volume as many smaller particles if they are pure acid droplets.

The ambient concentrations of H^+, sulfate (SO_4^{2-}), and ammonium (NH_4^+), collected on polycarbonate filters and measured as a function of particle size, were highest for particles with diameters between 280 and 530 nm, but the size distributions also suggested that a small peak of these ions existed in the particle size range below 88 nm. The H^+/SO_4^{2-} ratio was somewhat higher for particles below 88 nm, suggesting greater excess acidity for these small particles.

Our continuous monitoring showed that airborne concentrations of ultrafine particles varied substantially with time. The iron nanofilm detectors provided a time-integrated number concentration over several days or weeks. The counts on the detectors were relatively low for some of the sampling sessions, resulting in high statistical errors in calculations. Nonetheless, agreement of the mean values was remarkably good for some of the measurements. In future tests, longer collection times and new technologies, such as improved particle-charging methods for electrical precipitation samplers, could provide more efficient collection of particles onto the detectors, higher counts, and lower count-associated uncertainties. In general, concentrations of ultrafine particles determined by AFM analysis of the detectors in the MOI-EAS and UDM appeared to underestimate the total number concentration as determined by comparison samplers.

The ability to monitor airborne acidic particles provided by these iron nanofilm detectors enlarges the array of air quality variables that can be measured. This may help to resolve some of the outstanding questions related to causal relations between demonstrated health effects of ambient particles and particulate matter (PM) components.

INTRODUCTION

More than 90% of all airborne particles, when measured by number concentration, are generally found in nuclei less than 150 nm in diameter (Whitby et al 1972; US National Research Council 1977; US Environmental Protection Agency [EPA] 1996). These particles, on average, represent only about 0.5% of the total airborne particulate volume and mass (John 1993) and thus have not generally been regarded as important contributors to the toxic effects of inhaled ambient air. Yet recent evidence suggests they may have an important role in health decrements associated with ambient PM. It is unlikely that all components of PM are equally toxic. Candidates for especially active components are acidic particles (H^+), ultrafine particles, and soluble transition metals. Although there is toxicologic evidence consistent with known mechanisms of toxicity for all three candidates, only H^+ and ultrafine particles have produced effects at exposure levels that occur in ambient air (EPA 1996). Perhaps the most likely candidates are hybrids of H^+ and ultrafine particles (ie, acid-coated ultrafine particles). The study reported here evaluated a measurement system that could provide the first estimates of number concentrations of strongly acidic particles in size-resolved particles to which people are exposed.

NUMBER OF ACIDIC PARTICLES

In some studies that utilized multiple PM metrics in their regression analyses, the strength of association improved as size decreased from total suspended particles to PM 10 µm or less in aerodynamic diameter (PM_{10}) to PM 2.5 µm or less in aerodynamic diameter ($PM_{2.5}$) to SO_4^{2-}, the last being primarily within the $PM_{2.5}$ fraction of the aerosol (Ozkaynak and Thurston 1987; Thurston et al 1994). Analyses of associations between 1980 mortality rates and four measures of particulate air pollution in 98 US communities showed nonsignificant associations with total suspended particles and PM_{10}, and significant associations with $PM_{2.5}$ ($P < 0.01$) and SO_4^{2-} ($P < 0.001$) (Ozkaynak and Thurston,1987). On the basis of these analyses, Lippmann (1989) hypothesized that had H^+ been measured, the effect coefficient would be larger and the P value smaller. A more recent study (Lippmann et al 2000) indicated that the mass concentration of H^+, especially when nearly all of the measurements were below the lower limit of detection, was not likely to be a causal factor in mortality. These data did not address the issue of whether the number concentration of strongly acidic ultrafine droplets was associated with mortality.

Sulfuric acid and ammonium bisulfate, both strongly acidic, are important components of the fine and ultrafine particle fractions in the ambient atmosphere. Several reports have observed that ambient H^+ and SO_4^{2-} concentrations have associations with adverse health effects (Bates and Sizto 1987; Dockery et al 1993; Thurston et al

1994; Lippmann and Thurston 1996). Investigators who included strong acidity measurements in their monitoring of the ambient atmosphere found that acidity correlated with adverse health effects (Dockery et al 1989; Ostro et al 1991; Thurston et al 1994; Lippmann and Ito 1995). In other studies acidity strongly correlated with the prevalence of bronchitis symptoms and lung function decrements in children (Dockery et al 1996; Raizenne et al 1996). Additionally, Thurston and colleagues (1994) observed that of several particle characteristics, acidity had the highest relative metric strength of association with hospital admissions for respiratory problems and asthma in Toronto. The analysis by Samet and colleagues (2000a,b) of 90 US cities showed that the association between PM_{10} and mortality was strongest in the northeast, where H_2SO_4 aerosol concentrations were the highest. This finding may indicate a role for the acidic aerosol particles in mortality.

Ambient acidic sulfates exist in two forms: as acid dissolved in aqueous droplets and as a surface layer of acid on solid particles. Exposure to the first type of aerosol has been studied extensively in animal and controlled clinical studies. The second type of aerosol, which is formed by H_2SO_4 adsorption onto, or formation on, particles with large surface–volume ratios (such as the typical carbonaceous or fly ash particle) can be potent in altering various indices of response. H_2SO_4 droplets have been found to alter a number of aspects of pulmonary physiology, biochemistry, and structure in clinical studies (EPA 1996). However, the only effect observed in healthy volunteers at concentrations relevant to ambient exposures was altered mucociliary particle clearance from the lungs of nonsmoking adults (Leikauf et al 1984; Spektor et al 1989). The only other adverse effects noted at concentrations approaching environmental levels have been changes in pulmonary mechanics of asthmatic subjects (Koenig et al 1983, 1989; Utell et al 1983). To date, clinical studies of acid aerosols have not reported notable adverse effects; thus controversy surrounds the plausibility of the association of acid aerosols with adverse health effects in epidemiologic studies.

Chen and coworkers (1995) provided important evidence that the number concentration of acidic particles plays a role in cellular response. Guinea pigs were exposed to varying amounts of H_2SO_4 (50 to 300 $\mu g/m^3$ layered onto 10^8 ultrafine carbon core particles/cm^3) and to a constant concentration of acid (350 $\mu g/m^3$ layered onto 10^6, 10^7, or 10^8 particles/cm^3). All of these particles had diameters of approximately 90 nm, and the acid was adsorbed onto a carbon core. Indicators of irritant potency in macrophages harvested from the lungs of exposed animals clearly showed an increase either (1) when a constant dose of acid was divided into an increased number of particles or (2) when the acid dose was increased and the particle number concentration remained constant. Early work by Amdur and Chen (1989) suggested that number concentration was important for H_2SO_4 aerosol, and Hattis and associates (1987, 1990) named the concept *irritation signaling*. However, subsequent research of Chen and coworkers (1995) indicated that inhaled acid-coated particles much smaller than those discussed by Hattis and associates (1987, 1990) were capable of producing lung responses. Oberdörster and colleagues (2000) reported that nonreactive, low-solubility ultrafine particles did not appear to cause inflammation in young healthy rats. Thus it is important to be able to distinguish between the number of acidic ultrafine particles and the total number of ultrafine particles for epidemiologic studies. Previously, no measurement methods were available to obtain these important data.

TOTAL NUMBER OF ULTRAFINE PARTICLES

Toxicologic studies have shown that ultrafine particles with low solubility were significantly more inflammatory in the lung than were larger particles of the same composition (Driscoll 1994). This may be because ultrafine particles are more rapidly transferred to the interstitium than are fine particles of the same composition and they exhibit greater accumulation in the regional lymph nodes and the lungs (Oberdörster et al 1992, 1995a). On a theoretical basis, a greater number of particles deposited in the lung should result in greater potential for toxicity.

Evidence has begun to accumulate to support the hypothesis that the number of ultrafine particles that deposit per unit surface area of the epithelial lining of the human respiratory system is an important determinant in lung injury (Hattis et al 1987, 1990; Amdur and Chen 1989; Chen et al 1995; Oberdörster et al 1995b; Seaton et al 1995; Peters et al 1997b; Wichmann and Peters 2000; Penttinen et al 2001). Further, the resulting alveolar inflammation can provoke attacks of acute respiratory illness in susceptible individuals (Seaton et al 1995). In particular, the work of Peters and colleagues (1997a,b) and Wichmann and coworkers (2000) suggests that at ambient levels the number concentration of inhaled particles may be a more important determinant of the risk than mass of inhaled particles. In 27 adults with a history of asthma, the best correlation for decrement in peak expiratory flow rate was with the number concentration of particles with diameters between 10 and 100 nm (Peters et al 1997a). More recent evidence has also shown an association between human mortality and exposure to fine or ultrafine particles (Wichmann et al 2000).

The risk of exposure to ultrafine particles is important because nanometer-sized particles dominate air environments, both outdoors (EPA 1996) and indoors (Owen et al 1990, 1992; Kamens et al 1991), but this exposure is difficult to isolate using mass measurements. Some have suggested that the responses to PM cannot be associated with number concentration because the number does not always correlate with $PM_{2.5}$ mass. However, EPA concluded that a correlation between the total number concentration and total mass of fine particles might be expected if comparisons were made over periods of days (EPA 1996).

HYPOTHESIS

We hypothesized that the size-resolved number concentration of H^+ to which people are exposed could be measured by newly developed iron nanofilm detectors on which H_2SO_4 droplets produce reaction sites. To test the hypothesis, we asked the following questions:

1. Is the surface integrity of the detectors maintained under ambient conditions (eg, over the four seasons) in both rural and urban atmospheres?
2. Can the iron nanofilm detectors be deployed in particle samplers (specifically the MOI-EAS system and the UDM) to collect ultrafine particles and measure the number concentrations of total and acidic particles?
3. How will the amount of strong acid measured in particles smaller than 100 nm collected on a filter correlate with the number concentration of acidic particles measured by the iron nanofilm detectors?
4. Are the time-integrated number concentrations of ambient ultrafine particles determined by measuring particles deposited onto the iron nanofilm detectors comparable to number concentrations measured by commercially available real-time (continuous) monitors?

The iron nanofilm detectors, development of reaction sites, and procedures for microscopic analysis of the detectors have previously been reported (Cohen et al 2000).

METHODS AND STUDY DESIGN

There is no method by which the number concentration of ultrafine acid aerosols can be measured to provide direct comparisons with the proposed measurements of acid aerosols made with iron nanofilm detectors. Thus we collected field measurements to provide an indirect comparison by the following process:

1. The number concentrations of acidic particles and total ambient particles that penetrated the 100-nm cut size stage of an MOI were measured by precipitating the particles onto iron nanofilm detectors deployed in an EAS.
2. The results of these measurements were compared with the estimated number concentrations of acidic particles and total particles determined from detectors deployed simultaneously in a UDM, which provided an opportunity at low cost to collect particles in the ultrafine to fine range.
3. Simultaneous measurements were made of the size-fractionated mass concentration of strong acids in samples collected on the submicrometer collection stages of an MOI and on a filter, parallel to the EAS, which collected particles penetrating the MOI's 100-nm cut size.
4. The size-resolved number concentration of all ambient particles with a diameter of 300 nm or smaller was measured with an SMPS.

Nonreactive detectors (nanofilms without iron layer) were included in the MOI-EAS and UDM to obtain data for future analysis of size-resolved number concentrations. The measurements should be comparable to, though less detailed than, measurements made with a more complex system such as the SMPS, which combines an electrostatic classifier–condensation particle counter with computer controls for scanning and recording concentrations over a set of size ranges. The following sections describe each of these instruments.

IRON NANOFILM DETECTOR PERFORMANCE

The iron nanofilm detectors tested in this research were silicon chips (5 mm $\times$ 5 mm $\times$ 0.6 mm) coated with iron by vapor deposition. They were prepared by a commercial vendor (IBM Corp, Yorktown Heights NY). For the two batches used in these experiments, the iron layer was 21.5 or 26 nm thick. The detectors were stored in a nitrogen atmosphere except during exposure. A previous study (Cohen et al 2000) demonstrated that deposition of strongly acidic droplets, H_2SO_4 and ammonium hydrogen sulfate [$(NH_4)HSO_4$], onto these detectors resulted in reaction spots on the metal film that could be viewed topographically by AFM. Light spots on the color AFM scans indicate an elevated area on the detector surface. AFM of detectors on which H_2SO_4particles had been deposited showed clearly recognizable reaction sites that formed a central elevation with a surrounding halo (Figure 1). The ring formation has been previously noted on scanning electron microscopy as a characteristic of H_2SO_4 particles (Huang and Turpin 1996).

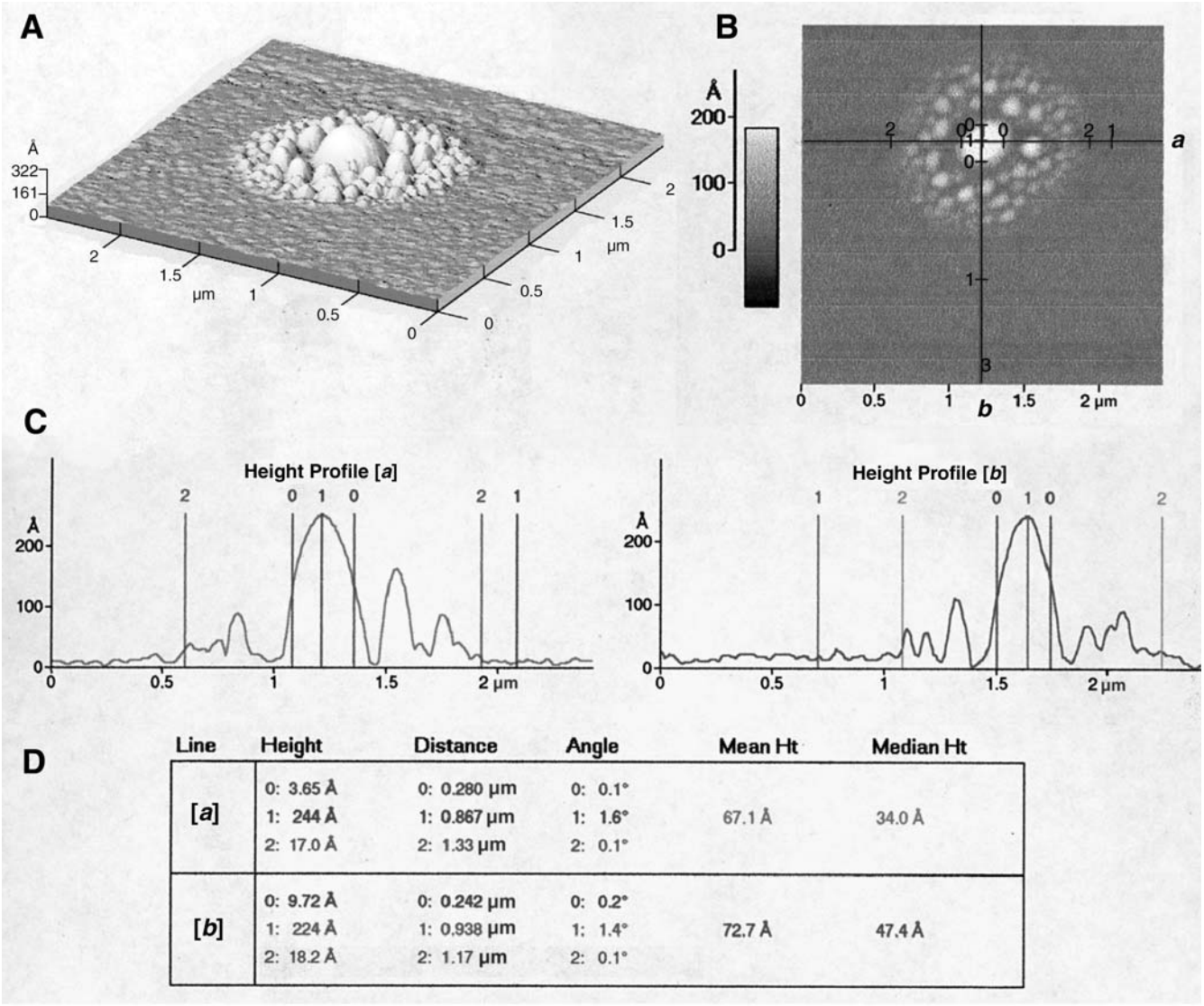

Line	Height	Distance	Angle	Mean Ht	Median Ht
[*a*]	0: 3.65 Å 1: 244 Å 2: 17.0 Å	0: 0.280 µm 1: 0.867 µm 2: 1.33 µm	0: 0.1° 1: 1.6° 2: 0.1°	67.1 Å	34.0 Å
[*b*]	0: 9.72 Å 1: 224 Å 2: 18.2 Å	0: 0.242 µm 1: 0.938 µm 2: 1.17 µm	0: 0.2° 1: 1.4° 2: 0.1°	72.7 Å	47.4 Å

Figure 1. Reaction site on iron nanofilm detector produced by an H_2SO_4 particle 141 nm in diameter. ***A.*** Three-dimensional representation of the reaction site. ***B.*** Two-dimensional representation of a reaction site showing measurement lines (*a* and *b*) for height. Light spots indicate elevated areas on the detector surface. ***C.*** Corresponding height profiles generated by the AFM along the lines shown on the two-dimensional image. ***D.*** Measures provided by the AFM for height and distance as differences between the indicated markers at different points along the lines. The height difference between the '1' markers indicates the peak height, and the distance measured between the "0" markers (full width at half maximum) indicates the peak diameter.

The surface roughness (about 5 nm) of the films was determined as an estimate of the standard deviation of the height of the undisturbed surface of the detector where there are no particles. This measure can be useful in judging the integrity of the detectors.

Calibration Aerosols

Test samples were prepared by depositing polystyrene latex (PSL) microspheres, sodium chloride (NaCl), and H_2SO_4 particles of known diameters onto the iron nanofilm detectors. For generating H_2SO_4 particles, dry filtered air was treated to remove particles, ammonia (NH_3), moisture, and organic compounds and passed over the surface of high-purity H_2SO_4 heated in a thermostat-controlled bath. The mixture was then passed through a thermostat-controlled, water-cooled condenser to form a nearly monodisperse aerosol (Xiong et al 1998). Three sizes of H_2SO_4 calibration standards were generated using a tandem differential mobility analyzer: 35, 64, and 141 nm. Monodisperse nonacidic aerosols were produced by nebulizing solutions

of NaCl (75 and 150 nm) or by dispersing PSL microspheres in ultrapure (18 MΩ) water, and selecting the desired size with an electrostatic classifier (model 3071, TSI, St Paul MN). The particle diameters (means ± SD) in the four PSL standard suspensions were 50 ± 2, 88 ± 8, 126 ± 4, and 198 ± 5 nm.

Calibration aerosols produced by one of the methods described above were passed into an EAS (model 3100, TSI) in which the particles were deposited on multiple iron nanofilm detectors. A subset of detectors was retained and subsequently exposed for 1 to 6 days to a different particle size.

A set of 5 calibration iron nanofilm detectors was used for quality control and scanned regularly to determine the effect of prolonged storage. Other sets were used to test the effects on the detector of elevated humidity and temperature and of ambient gases and vapors (see Tables 2 and 3). PSL microsphere samples were used for calibration of the atomic force microscope.

Response to Humidity and Temperature

Blank iron nanofilm detectors and a set of detectors that were previously exposed to H_2SO_4 calibration aerosols were placed for 3 months under storage conditions of high relative humidity (RH) at average and high temperatures (see Table 2): 92% RH at 22°C; and 88% RH at 39°C. The 3-month period was selected because we estimated that detectors might be used in the field for one full season. The detectors were scanned with AFM before and after the test and periodically examined visually during the course of the exposure. These tests were performed to verify the stability of the iron surface in extreme weather conditions occasionally experienced during summer in New York.

Response to Ambient Gases

During field sampling unexposed iron nanofilm detectors and detectors that were previously exposed to H_2SO_4 calibration aerosols were exposed to particle-free air by drawing filtered ambient air over them for the duration of the sampling period. This was to verify that the ambient gases did not have an adverse effect on the surface structure.

FIELD SAMPLERS

The field sampling system was an assemblage of individual sampling devices designed to simultaneously collect four to six different sets of data. Flow rates on all sampling systems were checked twice daily (morning and evening) during field sampling sessions, and weather conditions were recorded at the same time.

MOI and EAS

This combined sampling system (Figure 2) utilizes an MOI (MSP Technology, St Paul MN) and an EAS for separating and ensuring collection only of particles that are smaller than 100 nm onto the iron nanofilm detector. The MOI collects particles larger than 100 nm. Smaller particles remain in the airstream. The flow is then divided into two streams, one of which flows through the EAS. In the EAS particles are precipitated onto the detectors. Only particles smaller than 100 nm enter the EAS. The reaction spots on the detectors are counted to obtain the total number concentration of acidic (and other) nuclei mode particles. The other stream passes through a polycarbonate filter in parallel with the EAS on which the size-selected particles are collected for the same chemical analysis done on the filters at the MOI impaction stage.

MOI with Diffusion Denuders The MOI is an eight-stage cascade impactor. The lower four impactor stages use chemically etched jets with 900 or 2000 microorifices with diameters of 100 or 50 µm, respectively. The nominal aerodynamic diameter cut points at 30 L/min flow rate are 15,000 (inlet), 3200, 1800, 1000, 530, 280, 160, 88, and 57 nm. Polycarbonate filters 47 mm in diameter (Nuclepore Corp, Pleasanton CA) were used as impaction substrates. This type of filter has the advantage of low mass per unit area, low hygroscopicity, and low contaminant levels.

For these experiments the first three impactor stages were used only to remove the larger particles from the airstream. The center of the filters on these three impaction plates was coated with silicon grease to prevent particle bounce. The eighth stage was removed, so the acidic particles that passed on to the EAS or the polycarbonate after

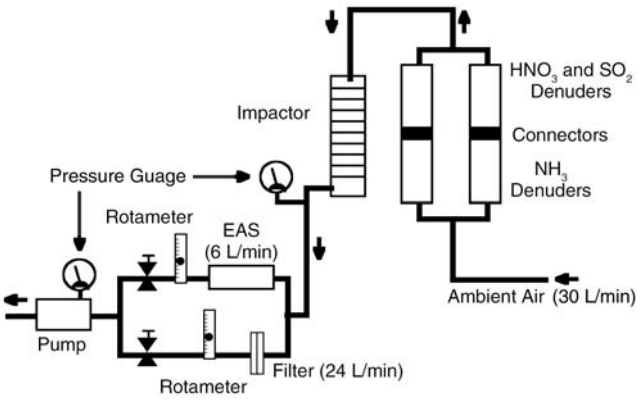

Figure 2. MOI-EAS sampler system. Twenty percent of the air flow from the MOI with particle diameters smaller than 100 nm continues to an EAS, in which the airborne particles are electrically precipitated onto iron nanofilm detectors. The remaining flow continues to a polycarbonate after filter for chemical analysis.

filter were below approximately 100 nm in diameter. Particles collected on the remaining stages were analyzed for H^+, SO_4^{2-}, and NH_4^+, which required extraction in aqueous solution and the use of ion chromatography; impaction filters for these stages were not greased.

Interstage losses of particles in the MOI previously were found to be 20% to 35% for particles with diameters larger than 3200 nm, below 2% for particles in the size range from 3200 down to 100 nm, and 5% to 10% for particles with diameters smaller than 100 nm (Marple et al 1991).

The average collection efficiency of the polycarbonate after filter was determined experimentally using laboratory-generated monodisperse NaCl particles of different sizes between 10 and 100 nm. Particles were generated from a NaCl solution using a Collison nebulizer and dried in a heating column before entering the electrostatic classifier, where a specific particle diameter was selected. At the exit of the electrostatic classifier, clean makeup air was added to the 3.0 L/min monodisperse aerosol to match the 24 L/min sampling flow rate through the filter. The concentrations of particles entering and exiting the filter were measured intermittently by a Faraday cup connected to an electrometer. The average polycarbonate filter collection efficiency was 76% ± 9% (mean ± SD), and this value was applied as a correction factor for the total mass collected on this filter.

Polycarbonate filters were also used as field blanks to be analyzed together with the filters used as MOI impaction substrates and the after filter. Three field blanks were used for each sampling session. In the laboratory each filter was put into a 47-mm filter holder and capped. At the sampling site the caps were removed at the beginning of the sampling session, and the blank filters were left in the uncapped holder next to the MOI during the entire session. At the end of the sampling session, the filter holder was capped and transferred to the laboratory together with the MOI. From that point on these blank filters were treated in the same manner as the field samples. The measurement results of the field blanks were used as background concentrations, which were subtracted from the field sample results, and in the determination of the lower limit of detection (LLD), defined as the smallest quantity or concentration of a chemical for which an analytical method will show a recognizable positive response. This was calculated as

$$LLD = 2 \times \sqrt{2} \times 1.645 \times S_b \,, \qquad [1]$$

where S_b is the standard deviation of the field blanks (Pasternack and Harley 1971).

Acid neutralization by ambient NH_3 and retention of gaseous nitric acid (HNO_3) and sulfur dioxide (SO_2) by sorption or reaction with the filter or the PM are known artifacts of particulate acidity sampling (Appel 1993). To minimize these artifacts, two sets of annular glass denuders (URG Corp, Carrboro NC) were placed in front of the MOI inlet. Each set contained two identical denuders. The denuders are 20.3 cm long and have an outside diameter of 2.2 cm. The diameter of the inner cylinder is 2.0 cm, which results in a 0.1-cm annulus. The first denuder in each set was coated with an ethanol solution containing 4.0 g of citric acid monohydrate and 3.0 g of glycerol per 100 mL of solution to remove NH_3 from the airstream (Koutrakis et al 1988). The second denuder in each set was coated with a 1:1 solution of methanol and water containing 1.0 g of sodium carbonate and 3.0 g of glycerol per 100 mL of solution to remove the gaseous HNO_3 and SO_2 from the airstream (Cheng 1995). Two sets of denuders were employed to increase the gas removal capacity.

The penetration efficiency (P) of gas through the denuder for the laminar flow regimen can be predicted from the empirical equation derived from a sorption study with SO_2 (Cheng 1995):

$$P = (0.82 \pm 0.1)\exp[(-22.53 \pm 1.22)\mu]$$

for $\mu > 0.02$ and $P < 10\%$,

$$\text{where } \mu = \frac{\pi DL(d_1 + d_2)}{4Q(d_2 - d_1)} \text{ and} \qquad [2]$$

D is the diffusion coefficient of the gas in cm^2/sec, L is the length of the coated area of the denuder in cm, Q is the flow rate through the denuder in cm^3/sec, and d_1 and d_2 are the inner and outer diameter, respectively, of the annulus in cm.

The calculated removal efficiencies ($1 - P$) of the denuders under the experimental conditions were 99.9%, 99.0%, and 98.0% for NH_3, HNO_3, and SO_2, respectively. Reported ambient measurements of these three vapors indicated maximum average daily concentrations in the eastern United States of less than 10 ppb for NH_3 (Cadle et al 1982; Haward et al 1982; Brauer et al 1991), less than 2 ppb for HNO_3 (Cadle et al 1982; Shaw et al 1982; Spengler et al 1990), and less than 5 ppb for SO_2 (Brauer et al 1991). At these levels, even under the highest daily average concentrations of these gases, penetration through the denuders would be 0.01, 0.02, and 0.1 ppb for NH_3, HNO_3 and SO_2, respectively. These concentrations would have an insignificant effect on the accuracy of the results.

The total collection capacity was calculated from the results of a chamber study of denuders with similar design and dimensions conducted by Brauer and colleagues

(1989). They determined that a total of 1 mg of gas or vapor can be collected on a denuder before a noticeable reduction in its collection efficiency. Assuming the maximum average daily concentrations in the eastern United States noted previously, the maximum sampling time calculated for each of the vapors for our sampling conditions was 78 hours for NH_3, 106 hours for HNO_3, and 42 hours for SO_2. As the shortest maximum sampling time was that of the SO_2 (42 hours), we replaced the denuders every 24 hours to provide significant safety margins.

The loss of ultrafine particles through the annular denuders used in this work was tested with laboratory-generated monodisperse NaCl aerosol. At the design flow rate (15 L/min), losses through the two denuders in series averaged 1.3% ± 2.2% for particles from 20 to 160 nm in diameter. The results of these tests are in agreement with the results of particle loss tests through a similar annular denuder carried out by Possanzini and associates (1983).

The denuders were set in a vertical position to avoid deposition of large particles on the denuder walls by sedimentation. In addition, preliminary data from ambient aerosol sampling at the sampling site indicated that the number concentration of particles with a diameter larger than 100 nm was normally very low.

EAS The EAS is an electrostatic precipitator with two stages, one charging and one collecting, that is designed to collect particles in a random and uniform manner onto a collection surface (2.5 cm × 12.7 cm). For this study the iron nanofilm detectors were placed over the collection area of the EAS to obtain uniform particle deposits. Uniform deposition was confirmed in prior experiments (Cohen et al 2000). The fraction of the particles that precipitate in the charging section is known to depend on particle size, but it is a reproducible number for most aerosols. The collection efficiency has been reported as 69% for 103-nm particles, about 60% for 28-nm particles, and about 50% for smaller particles (Liu et al 1967). The collection efficiency is relatively low because not all of these very small particles can acquire an electric charge during the time they reside in the charging section. The particle collection efficiency of the EAS (E) was confirmed experimentally for different particle sizes using monodisperse PSL microspheres.

Ultrafine Diffusion Monitor

The UDM, a low-flow diffusion monitor developed in our laboratory for the collection of time-integrated samples of ultrafine ambient particles, is a flat, rectangular aluminum channel 1.0 mm high and 50 mm wide (Figure 3). The monitor has depressions cut to hold multiple detectors flush with the inner surface. The first two units we made were 500 mm in length. For outdoor sampling the inlet of the UDM penetrated a slit cut through the wall of a steel hood in which the UDMs were housed and extended about 5 inches from the outer wall. A Plexiglas rain shield protected the inlet from above. Air was drawn through the monitor by a low-flow pump. The particles entering the monitor deposited by diffusion onto the walls of the channel. Two iron nanofilm detectors and one nonreactive silicon detector were placed side by side, in the cut receptacle, on the lower wall, at 7.0, 201.5, and 452 mm (midpoint of detector) from the inlet along the length of the channel. The nonreactive detector was used to collect a sample of ultrafine particles, and the iron nanofilm detectors were used to quantitate both the total number of particles and those particles that were acidic. We initially used one UDM sampler at a flow rate of 10 cm^3/min. In the winter sampling session, a second UDM with a flow rate of 200 cm^3/min was added, and both were used for subsequent sampling sessions. Although the deposition efficiency was reduced at the higher flow rate, the increased volume of air sampled provided more deposited particles.

We did two pilot experiments in which both outdoor and indoor air was sampled. For each we made a new UDM that was 95 mm in length with detector receptacles centered at 12.5 and 47.5 mm from the inlet. The flow rate for both was 200 cm^3/min.

The integrated air concentration of both acidic and nonacidic particles can be calculated from the known deposition efficiency as a function of particle size at different locations in the sampler and the flow rate. The deposition efficiency of particles decreases with increasing distance from the inlet, so fewer particles will be found on detectors placed farther from the inlet.

The deposition efficiencies of ultrafine particles along the channel have been predicted by stepwise calculations using the equations for diffusion of particles in rectangular

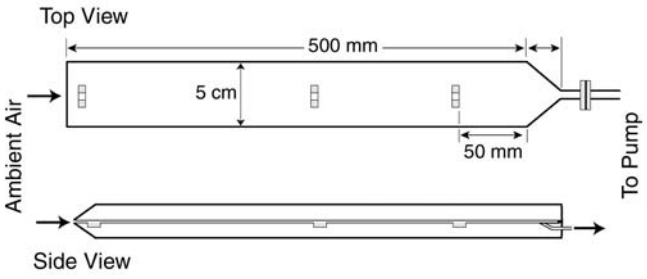

Figure 3. Schematic of the UDM. Sets of three blank detectors (one bore silicon and two iron nanofilm) were placed along the channel at different distances from the monitor inlet. Flow rate (Q) = 10 or 200 cm^3/min.

channels (Hinds 1982). The penetration efficiency (*P)* of particles through rectangular channels is given as

$$P = 1 - 2.96\ \mu^{2/3} + 0.4\ \mu, \text{ for } \mu < 0.003 \quad [3]$$

$$P = 0.910\ \exp(-7.54\ \mu) + 0.0531\ \exp(-85.7\ \mu) + 0.0153\ \exp(-249\ \mu), \text{ for } \mu > 0.003, \quad [4]$$

where μ is the deposition parameter, calculated as μ = *DLW/Qh,* and *D* is the diffusion coefficient of the particle (cm^2/sec), *L* is channel length (cm), *W* is channel width (cm), *Q* is flow rate (cm^3/sec), and *h* is channel height (cm).

The deposition efficiency of particles on the walls of the UDM was experimentally determined with monodisperse fluorescein particles with diameters of 50 and 100 nm using aluminized Mylar as a collection substrate. A few confirmatory experiments were carried out in a radon chamber with both unattached and attached radon progeny (approximately 3 and 90 nm in diameter, respectively). Uniform deposition across the width of the monitor wall has also been verified. Deposition was measured for various flow rates and locations in an earlier version (a widening channel diffusion monitor). For each of these monitors, the measured deposition efficiencies on a collector (10 mm × 50 mm) centered at the location of the detector receptacles were greater than those predicted for the detectors located closest to the entry, probably because of entrance effects on the flow into the sampler. Efficiency values at the rear location (near the end of the air channel) showed better agreement.

SMPS

The SMPS counts the number of particles per cm^3 of air in a series of size ranges. It includes an electrostatic classifier (model 3071, TSI), a condensation particle counter with a fast scanning EPROM chip (model 3010-S, TSI), and an impactor with a 0.7-μm cut size (at 1 L/min) placed before the aerosol inlet of the classifier. The system is operated in scanning mode with SMPS software (model 390088, TSI). In this study size distribution was measured every half-hour by averaging three scans for each measurement. The particle size range was from 7 to 300 nm in 32 size bins. Because the instrumentation has to be kept indoors, the inlet is through insulated stainless steel tubing (9 m long, 0.635 cm in diameter).

CNC

A CNC (model 3020, TSI) monitored the number concentration of airborne particles throughout each sampling session. The inlet tube (10 m long, 0.635 cm in diameter, flow rate of 300 cm^3/min) was adjacent to the SMPS inlet. A chart recorder was used to collect the number concentration data. These real-time data were useful for range finding, allowing us to estimate surface deposition on the detectors in the EAS. Data were collected to compare with the SMPS data as an accessory quality control measure.

Filtered Air Canister

To test whether ozone or other reactive components of the atmosphere may affect the iron nanofilm detector surface, detectors previously exposed to calibration acid aerosols and blank detectors were exposed to ambient gases and vapors. This was accomplished by placing one detector exposed to calibration acid aerosols and one blank detector in a sealed aluminum canister (2.45 cm high, 7.9 cm in diameter, 120.1 cm^3 volume) with a membrane inlet filter (Millipore GS, 0.22-μm pore size). The inlet opening was 0.5 cm in diameter. Air was pumped through the canister at 50 cm^3/min. Detectors were changed each week.

FIELD SAMPLING SITES AND SESSIONS

The sampling sessions are listed in Table 1. Each set of measurements affords only an average sample that provides evidence that accurate measurements can be obtained with the new detection system. Outdoor temperature, RH, barometric pressure, and weather conditions were monitored and recorded.

Rural Outdoor Site: Tuxedo NY

To obtain four sets of comparative measurements, outdoor sampling was scheduled for two 1-week sessions during each of the four seasons at a rural site in Tuxedo NY, starting in summer 1999. This schedule was selected to obtain a reasonable variety of ambient field conditions and achieve confidence in the performance of the detectors outdoors under different weather conditions. An extra week was added to the fall session in order to obtain a 2-week UDM sample (fall 2+3).

All of the particle samplers were deployed at the Tuxedo site: that is, (1) the MOI, to collect particles in size-segregated classes, with two branches (the EAS and polycarbonate filter) that collect particles less than 100 nm in diameter; (2) the two UDMs; (3) the SMPS system, to count particles with diameters less than 300 nm in 32 size bins; and (4) the CNC, to determine the total number concentration of particles; and (5) the filtered air canister, a gas-phase sampling unit containing test detectors.

The MOI-EAS, UDMs, and filtered air canister (all containing iron nanofilm detectors) were placed within a

Table 1. Field Sampling Sessions

Sampling Session	Dates	Weather	Temperature (°C)	Barometric Pressure (mm Hg)	Relative Humidity (%)
Outdoor					
Summer 1	07/14–07/21/1999	Hot and humid, some haze, occasional thundershowers	22–36	740–748	24–76
Summer 2	07/21–07/28/1999	Hot and humid, some haze, mostly sunny, 2 partly cloudy days	21–36	735–743	24–88
Fall 1	10/21–10/28/1999	40% sunny, 60% cloudy	0–17	729–752	35–100
Fall 2	10/28–11/04/1999	Equal time fair, cloudy, 1 day rain	1–24	731–754	34–100
Fall 3	11/04–11/11/1999	6 days fair, 1 day cloudy	−1–22	737–750	20–100
Winter 1	02/01–02/08/2000	Clear, cloudy, snow	−11–4	735–752	24–92
Winter 2	02/08–02/16/2000	Rain, cloudy, fair, light snow	−11–10	731–747	25–100
Winter 3 (NYC)	03/09–03/16/2000	Drizzle, overcast, clear and sunny, some rain	1–31	752–771	16–67
Winter 4 (NYC)	03/16–03/23/2000	Overcast, rain, clear and sunny, windy drizzle	−3–23	757–778	16–90
Spring 1	05/01–05/08/2000	Cloudy, rain, sunny, cloudy	6–36	735–749	20–100
Spring 2	05/08–05/15/2000	Thunderstorm, cloudy, sunny, rain, cloudy, sunny	7–33	733–744	26–100
Indoor					
NIEM cafeteria	08/03–08/10/2000	Sunny, partly cloudy	23–28	738–741	47–60
Newburgh residence	09/07–09/18/2000	Partly cloudy, hazy, fog, clear	10–27	757–776	45–100

custom-built 3-foot-square stainless steel unit that stood 1.5 feet off the ground, to protect them from the elements (Figure 4). A 4-inch-diameter stainless steel duct extended 2.5 feet above the slanted roof. Air samples were drawn from the duct through ports located within the hood. Two thermostat-controlled fans on the floor drew air into and out of the unit to prevent overheating in the summer. In addition, these fans ensured that the impactors' operating temperature was the same as the ambient temperature. Temperature differences between the impactor and the ambient air can cause evaporation or condensation that distorts the particle size distribution. To reduce any effect of the nearby building on the sampling process, the stainless steel unit was placed approximately 30 feet away. A small infrared lamp was used in the unit during the winter sessions to maintain the temperature in the operating range for the UDM and filtered air canister pumps.

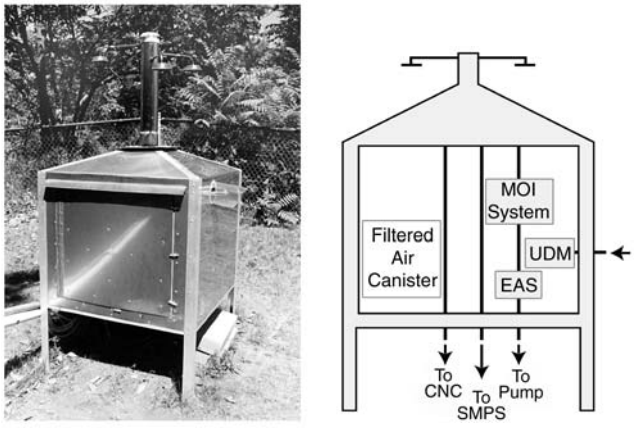

Figure 4. Stainless steel unit to protect outdoor samplers. ***Left panel.*** Exterior view of unit, which housed the MOI-EAS system, the UDM, and the filtered air canister (a gas-phase sampling unit containing test detectors). Other inlets had tubes leading to the SMPS and CNC, which were deployed in a nearby shed, along with electronic components and large pumps. ***Right panel.*** Schematic of the housing unit.

The CNC, SMPS, and large electronic pumps were housed inside a shed adjacent to the stainless steel unit. A heating system was installed in the shed to maintain the temperature within the operating range required for the electronic equipment (15°C to 24°C).

Urban Outdoor Site: New York City

To seek possible artifacts caused by source differences in a heavily populated urban area, we also sampled for two 1-week sessions in New York City (winter 3 and winter 4). Winter sessions were selected because we expected many local ultrafine particle sources from heating systems. All of the samplers that were deployed in Tuxedo were moved to New York City.

The sampling site was on the roof of a 14-story dormitory building at the NYU Medical School on First Avenue at 31st Street in Manhattan. Sampling inlets with individual rain shields were located 6.5 feet above the roof and placed 9, 12, and 14 feet from a roof utility shed, which housed the MOI-EAS, SMPS, and CNC. Stainless steel air-sampling lines were brought into the shed through penetrations near its roof. A large rainproof metal case was placed on a cart about 5 feet from the roof shed. The case held the filtered air canister and the two UDMs, with their inlets penetrating small slits open to the environment. The box also housed the low-flow sampling pumps. Another case held the thermometer and RH monitors.

Indoor Sites: Tuxedo and Newburgh NY

Indoor tests were conducted in the cafeteria at the Nelson Institute of Environmental Medicine in Tuxedo (August 3 to 10, 2000) and in a residence in Newburgh NY (September 7 to 18, 2000). Sampling for both of these sites was limited because of the inconvenience to occupants. Because outdoor infiltration may be an important source of indoor airborne particles, concurrent indoor and outdoor sampling was carried out with the UDMs at both sites. Relevant data, such as activities in the test environment, identifiable indoor sources, weather conditions, indoor and outdoor temperatures, pressure, and RH, were recorded in a sampling log. As the objective was to document comparative responses of the sampling systems, full characterization of ventilation, infiltration, and other particle sources and sinks was not necessary.

At the NIEM cafeteria, only the two UDMs, filtered air canister, SMPS, and CNC were used; the MOI-EAS was not used. One UDM sampled indoors and one sampled outdoors. A switching valve was timed to draw either an indoor or an outdoor sample into the SMPS every 15 minutes; thus each environment was sampled every half hour as for the previous experiments. The inlet valve switched immediately after completion of three scans on the SMPS to allow time for the lines to flush with the appropriate sample air before recording size-selective concentrations of the next sample. The CNC sampled only indoor air.

At the Newburgh residence, only the two UDMs and the filtered air canister were used. One UDM was placed indoors in a dining area. The other was placed on an adjacent screened porch that had no mechanical ventilation and was essentially a sheltered outdoor space.

SAMPLE HANDLING AND ANALYSIS

Iron Nanofilm Detectors

After exposure the iron nanofilm detector surface was scanned topographically by AFM to view and enumerate the reaction sites. The reaction sites produced by acidic and nonacidic particles differed (Figure 5). Collected particles and reaction sites on each detector were sized and counted on the image obtained with an atomic force microscope (Autoprobe CP System, Thermomicroscopes, Sunnyvale CA) in noncontact mode using ultralever tips (Cohen et al 2000). Specifically, one location in each of the four quadrants of the detector surface (5 mm × 5 mm) was chosen at which to make contact with the tip. When the tip neared contact with the sample, an area of 200 µm × 200 µm was available for scanning. This area was divided into 16 equal squares (25 µm × 25 µm) that were numbered from 1 through 16. Four of the 16 squares were then selected using a random number list. The central area

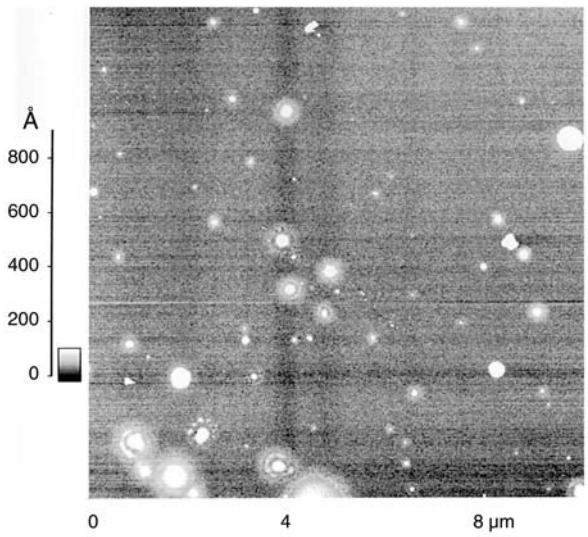

Figure 5. Image of a scan of an iron nanofilm detector exposed in the MOI-EAS for 2 days in summer 1 sampling session. The ringed reaction sites produced by acidic particles are clearly different from the sites produced by nonacidic particles.Tuxedo NY outdoor: 48 hr, July 14–16, 1999, 10 µm × 10 µm.

(10 μm × 10 μm) in each of the selected squares was then scanned. Collected particles and reaction sites were thus counted by scanning a total of 16 fields of 100 μm^2 each.

Because of the enormous counting effort required for these experiments, we altered the protocol as follows: If it was clear that a total of 200 particles would be detected in four scan areas, then only two scans (total area, 400 μm^2) were done in each of two different quadrants of the detector. A count of 200 particles resulted in an acceptable Poisson counting error of 7%. For samples with lower particle counts per 100-μm^2 area, eight scans, four in each of the two quadrants, were counted. Blank samples were scanned over the duration of the experiments.

Noncontact AFM is one of several techniques in which the cantilever is vibrated near the surface of the sample. The space between the tip and the sample is on the order of tens to hundreds of angstroms—in the range of attractive van der Waals forces. As noted previously, the H_2SO_4 reaction sites were clearly recognizable morphometrically by a ring around the particle. However, we did observe some sites without detectable rings on film surfaces exposed to standard acidic particles. This is because AFM scan parameters and techniques influence the amount of detail that can be distinguished. The halos were much more evident, for example, on a scan of 64-nm standard particles (Figure 6A) than on a scan of 141-nm standard particles (Figure 7A). These differences in detail may have resulted in an underestimate of the number concentration of ambient acidic particles.

For quality control a calibration grating was scanned once each week, and iron nanofilm and nonreactive detectors exposed to known calibration aerosols were scanned once a month. Since the counting area was only 10 μm on each side, it was not possible to locate the same spot with the AFM tip for repeat analyses. Field blanks were included for each sampling session. Laboratory blanks accompanied each batch. As a further check on the surface integrity of the iron nanofilm after exposure, we examined apparently clean areas on the scans for any increase in surface roughness.

The number of particles per scan was counted directly on the image displayed by the atomic force microscope. Particle size can be measured either directly by the AFM Proscan imaging program or by importing the image into Image SXM, an extended version of the public domain image analysis software NIH Image, but was not determined in this study. Both the total number of particles and the number with halos were recorded. The halos were assumed to be caused by deposition of strongly acidic particles. A

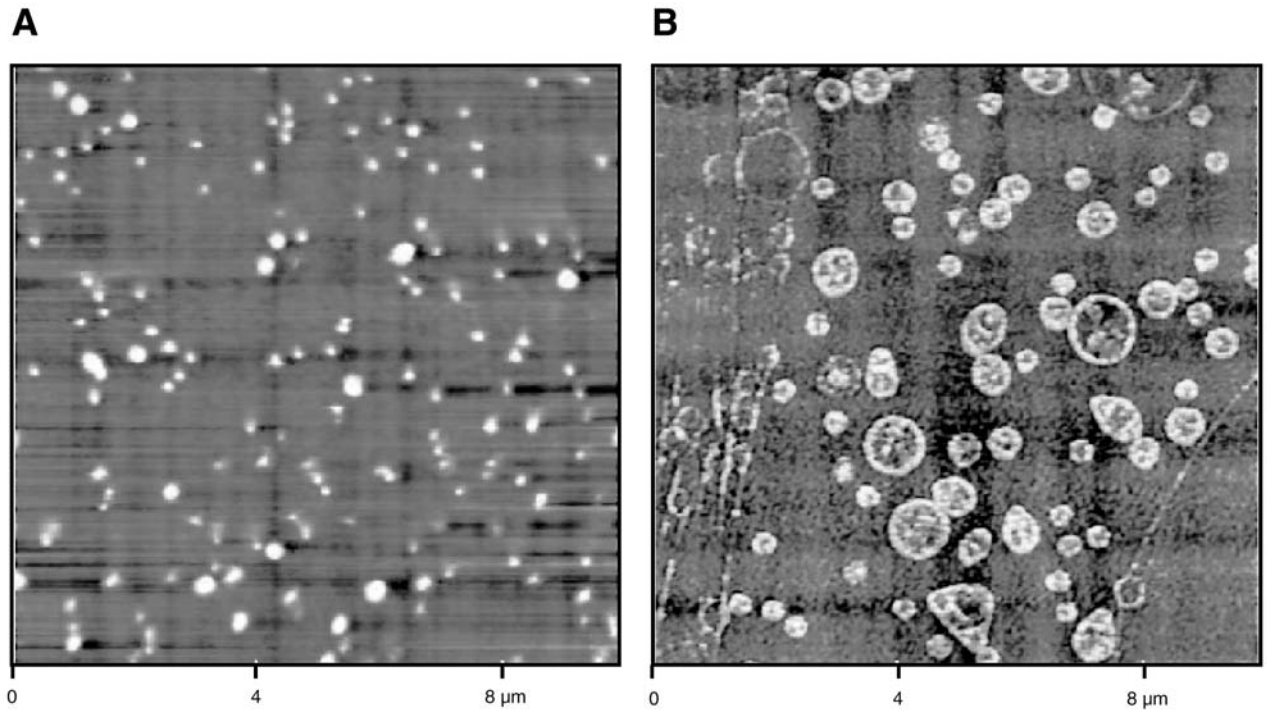

Figure 6. Iron nanofilm detector exposed to 64-nm H_2SO_4 particles. ***A.*** Image of a scan immediately before storage. The ring formations are evident. ***B***. Scan of a different area on the same detector after storage for 3 months at 88% relative humidity and 39°C.

value of 2 particles per scan area was subtracted for nonreactive particles for all sample calculations; this value was based on a long-term average of 2 ± 3 particles per scanned area (10 µm × 10 µm) of blank samples. No acid reaction sites were ever detected on a blank sample (data not shown).

At the conclusion of a field sampling session, the iron nanofilm detectors and uncoated silicon detectors were removed from the EAS, the UDMs, and the filtered air canister. Until AFM analysis, the detectors were stored in a sealed tray placed inside a desiccator that was purged with high-purity nitrogen and sealed.

MOI-EAS Detectors The particle number concentration (C, in particles per cm^3) can be calculated from the count on a specific microscope field corrected for deposition efficiency:

$$C = N/nA_s hE_f, \quad [5]$$

where n is the number of collector square-wave (alternating voltage) cycles; A_s is the area of the microscope field; h is the height of the sampling chamber above the sampling surface (used to calculate the volume of air from which the particles are precipitated); E_f is the efficiency of particle deposition for the sampler; and N is the number of reaction sites, or particles, per microscope field.

The experimental deposition efficiency (E_f) for the three different sizes of PSL standards, 50 nm, 126 nm, and 198 nm, was 0.63 ± 0.08, 0.78 ± 0.09, and 1.02 ± 0.09, respectively. The results are consistent with what Liu and coworkers (1967) obtained, except our value was somewhat higher for the 198-nm particles. For these experiments, which collected only particles that penetrated the 100-nm cut size of the MOI, we used an average deposition efficiency value of 66%.

UDM Detectors We did not size the deposited particles or acid reaction sites for these experiments but estimated the total number of ultrafine particles deposited on the iron nanofilm detectors in UDMs by scanning areas on which particles with diameters less than 200 nm were visualized. Larger particles were rarely observed.

The deposition efficiencies for particles from 7 to 300 nm in diameter at the detector locations in the UDM were calculated using the equation for diffusional particle deposition in rectangular channels at the average flow rate measured during each sampling session (Hinds 1982). The deposition efficiency on the scan area was then corrected by the ratio of the area used for the calculation to the 100-$µm^2$ scan area.

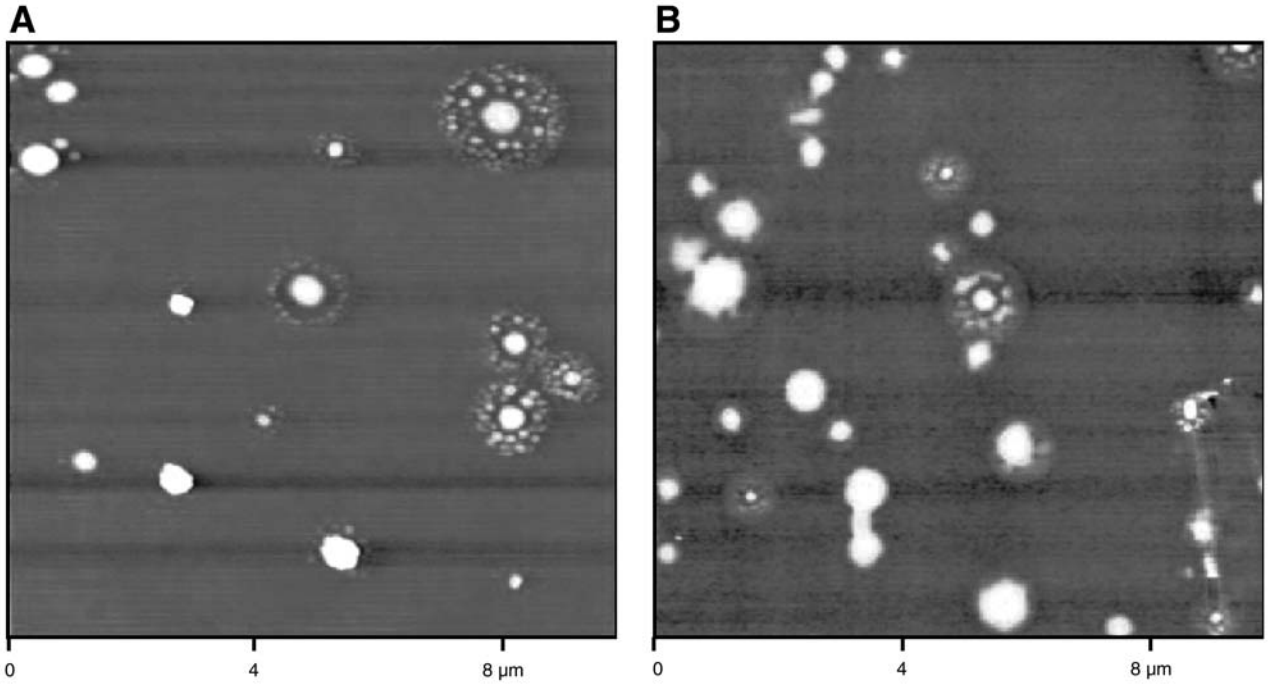

Figure 7. Iron nanofilm detector exposed to 141-nm H_2SO_4 particles. ***A.*** Image of a scan immediately before exposure to ambient air. ***B.*** Scan of a different area on the same detector after exposure to particle-free ambient air in the filtered air canister for 1 week.

The estimated average deposition efficiency was applied to calculate the concentration of ultrafine particles in air. The detector samples have been archived and may be scanned in the future to obtain the particle size distribution. The particle size distribution in air can then be calculated using the known deposition efficiency of each particle size.

The airborne concentration (C, in number per cm^3), represented by the deposited particles, is calculated as

$$C = N/EV, \quad [6]$$

where N is the net average number of particles counted per 100 μm^2; E is the deposition efficiency on the scan area; and V is the volume sampled (cm^3).

Filtered Air Canister Detectors Iron nanofilm detectors exposed to calibration acid aerosols and blank detectors were scanned by AFM before and after exposure in the field to document the surface roughness of the nanofilm and the diameter of the acid reaction sites. The detectors were visually observed for obvious deterioration of the surface when they were removed from the air canister.

MOI Filter Samples

After a sampling session was completed, the MOI impactor was disconnected from the pumps, and both the inlet and outlet ports were capped to avoid neutralization by ambient NH_3. The impactor and the bypass filter were then transferred to the laboratory. In the laboratory the polycarbonate filters were removed in an NH_3-free hood, and each was stored in a capped 5-mL conical tube. The same tube was later used for extracting the filter. All the capped tubes were then stored inside a sealed glass jar that was lined with filter paper coated with citric acid. This protected the filters from neutralization by NH_3 prior to their analysis.

The ion analyses of all filter samples, together with field and laboratory blanks and positive (spiked) controls, involved the application of two methods: (1) determination of the aerosol acidity (H^+) via the pH method developed by Koutrakis and colleagues (1988); and (2) determination of nitrate, sulfate, and ammonium ions by ion chromatography.

Briefly, the pH method involved the extraction of the sample in 3 mL of 10^{-4} M perchloric acid ($HClO_4$) and 0.04 M potassium chloride (KCl) for ionic strength. A pH meter was used (model 611, Orion Research, Beverly MA). The H^+ concentration of the extract was calculated and then converted to equivalent H_2SO_4 concentrations using a calibration curve generated from a known dilution of certified 1 N H_2SO_4 solution (Fisher Chemical, Fair Lawn NJ). This analysis method is more sensitive than older methods because the aerosol sample is extracted into a small volume of extraction solution and a microelectrode is used for the pH determination.

Nitrate, sulfate, and ammonium ion concentrations were determined via an ion chromatograph (model DX-500, Dionex Corp, Sunnyvale CA) coupled with a conductivity detector (CD 20, Dionex Corp). Calibration curves for the ion chromatographic analysis were generated using a known dilution of NIST-certified 1000 ppm (1000 µg/mL) standards (Spex CertiPrep, Metuchen NJ). The separator columns we used were AS4A for anions and CS3 for cations. The eluants used were 1.8 mM sodium carbonate (Na_2CO_3) and 1.7 mM sodium bicarbonate ($NaHCO_3$) for anions, and 42.5 mM methanesulfonic acid (CH_3SO_3H) for cations. During the ion chromatographic analysis, a random standard was chosen and run as unknown after every six samples to verify the validity of the calibration curve and ensure the proper operation of the instrument. The results were immediately evaluated for acceptability. When a sample's concentration exceeded the range of the calibration curve, a series of dilutions were made to bring the concentration down to approximately the center of the range.

SMPS Analysis

Particle size spectra were all corrected for transport losses through the 9-m-long inlet tubing as estimated from diffusion theory (Hinds 1982). The estimated penetration fraction for particles of 30, 70, and 100 nm was 0.89, 0.96, and 0.97, respectively (Figure 8). The average particle size distribution was plotted for each 24-hour period and for the duration of the each sampling session. In addition, for

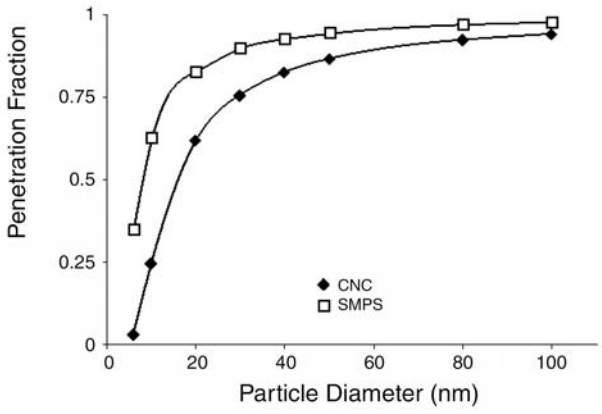

Figure 8. Calculated penetration of particles through inlet tubing used during outdoor sampling at the Tuxedo site. The CNC tube was 10.0 m long with flow rate of 300 mL/min; the SMPS tube was 8.8 m long with flow rate of 1 L/min.

comparison with the number concentrations measured by the detectors from the MOI-EAS and from the UDMs, particles with diameters between 35 and 100 nm and between 40 and 300 nm, respectively, were counted and averaged over the appropriate sampling duration.

The hourly average number concentrations accumulated overall particle sizes were also calculated for comparison with the number concentrations measured by the CNC.

CNC Analysis

The chart recordings of particle concentration as a function of time were scanned visually, and hourly averages were obtained. These values were plotted to display the average hourly concentration in particles per cm^3. Calculated penetration through the CNC inlet tubing is shown in Figure 8 together with that for the SMPS inlet.

RESULTS

DETECTOR ANALYSIS

We used PSL microspheres with diameters of 50 ± 2 nm, 88 ± 8 nm, 126 ± 4 nm, and 198 ± 5 nm to verify calibrations of the atomic force microscope. The height measurements (*z* calibration) showed a very good fit to the nominal diameters of the PSL microspheres (Figure 9). The diameter measurements (*x* calibration) were more problematic. Several factors affect size analysis with AFM. The resolution of distance (*x*) depends on the height (*z*) of the object as well as on the width and shape of the microscope tip. Thus, especially for objects in the nanometer size range, the variability in size and shape of the tips that results from manufacturing can strongly influence the resulting measurements (Figure 10). In our system particles with diameters down to 50 nm could be counted, but not accurately sized. We showed previously (Cohen et al 2000) that the acid reaction sites were about 3 times larger in diameter than the airborne particles; thus we could resolve smaller acidic particles than we could nonreactive particles.

DETECTOR PERFORMANCE

Control Samples

The results of monthly quality control measurements are shown in Figures 11, 12, and 13, in which each curve represents the measurements of surface roughness on one iron nanofilm detector followed for approximately 18 months and scanned approximately once a month. The measurements made on three detectors stored under nitrogen at room temperature demonstrated that the detector surface was very stable for both the one blank detector and the two detectors previously exposed to acid standards. Figure 11A shows the average roughness in a

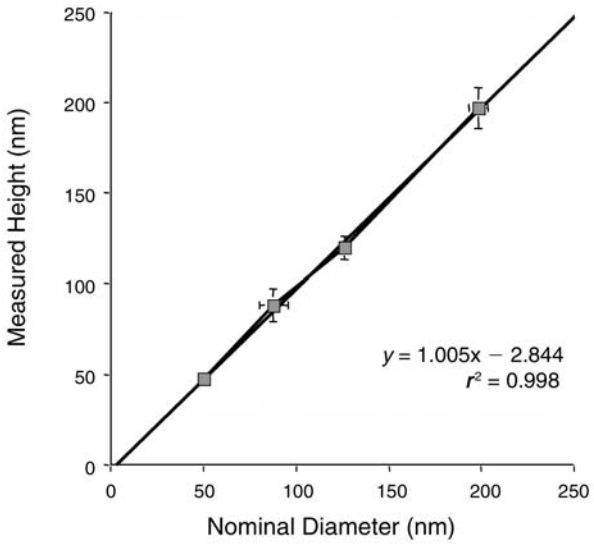

Figure 9. Height of PSL microspheres indicated on an AFM scan compared with nominal diameter (*z* calibration). Good correlation is indicated between the height and nominal diameter of the particles. The vertical error bars represent 1 SD of the replicate measurements; horizontal bars are the SD of the nominal diameter provided by the supplier of the PSL microspheres.

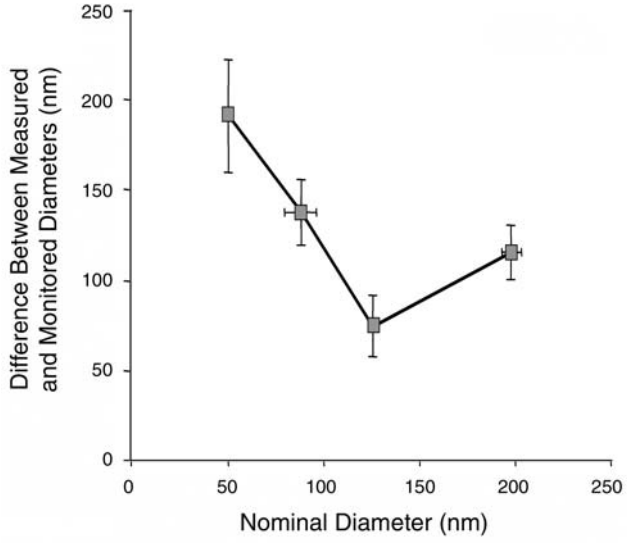

Figure 10. AFM scan indicated dimensions of PSL microspheres compared with nominal diameter. Note the lack of correspondence between the nominal diameter and the diameter measured in the plane of the surface. The vertical error bars represent 1 SD of the replicate measurements; horizontal bars are the SD of the nominal diameter provided by the supplier of the PSL microspheres.

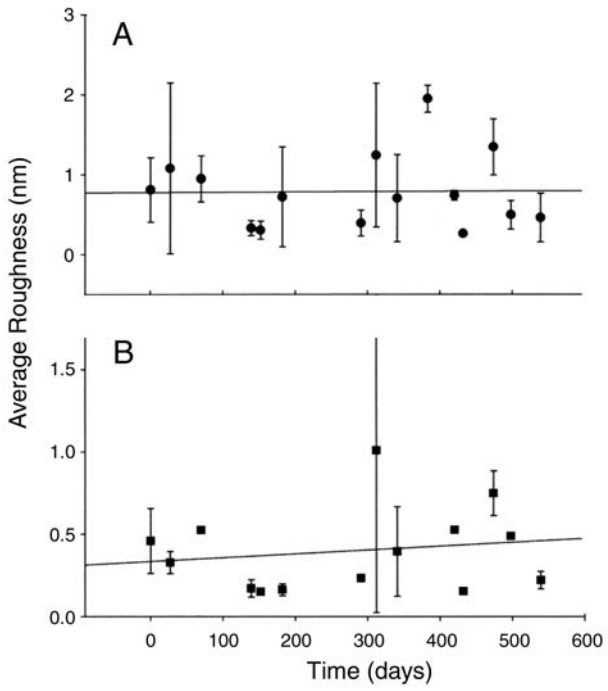

Figure 11. Average roughness of a blank quality control detector over time. ***A.*** Each point represents an average of four scanned areas (each 100 μm^2), two in each of two quadrants. ***B.*** Zoomed scan area; each point represents an average of two scanned areas (each of roughly 2.5 μm^2), one in each of two quadrants. Vertical bars represent 1 SD of the replicate roughness measurements.

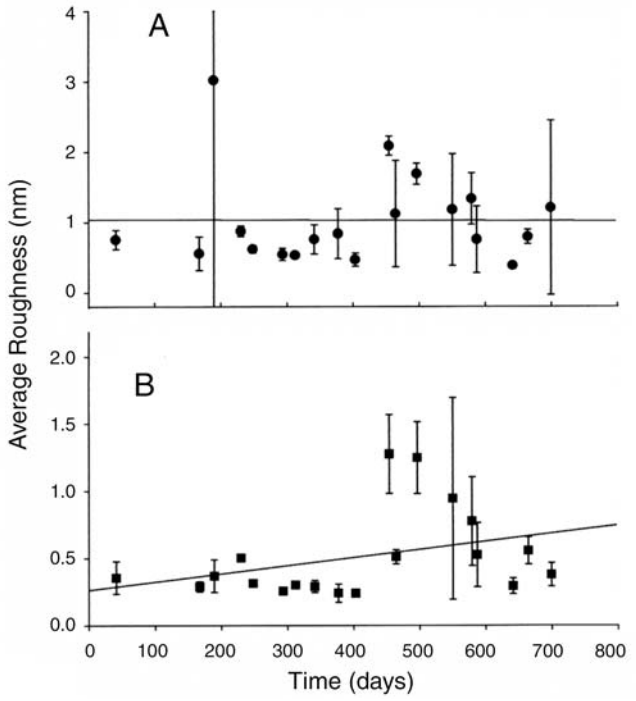

Figure 12. Average roughness over time of a quality control detector exposed to 64-nm acidic particles. ***A.*** Each point represents an average of four scanned areas (each of 100 μm^2), two in each of two quadrants. ***B.*** Zoomed scan area; each point represents an average of two scanned areas (each of roughly 2.5 μm^2), one in each of two quadrants. Vertical bars represent 1 SD of replicate roughness measurements.

100-μm^2 area on the blank detector as a function of time. The regression equation for the roughness is $0.78 + 4.4 \times 10^{-5}$ nm × Time ($r^2 = 2.8 \times 10^{-4}$). Figure 11b shows the same parameter for a region of approximately 2.5 μm^2 selected to be free of particles. The regression equation is $0.34 + 2.4 \times 10^{-4}$ nm × Time ($r^2 = 0.028$). The average number of particles counted (± SD) per 100-μm^2 area over 18 months was 5.7 ± 2.9. As judged by many detector measurements over the duration of the experiment, this blank quality control detector had a somewhat higher number of particles counted and a somewhat rougher surface than the average detector, but both measures were exceedingly stable.

The average surface roughness over time was also determined for the two acid-exposed detectors. The regression equations for the roughness of a detector initially exposed to acidic particles 64 nm in diameter (Figure 12) are $1.0 - 2.9 \times 10^{-5}$ nm × Time ($r^2 = 7 \times 10^{-5}$) for a 100-μm^2 area and $0.26 + 6.07 \times 10^{-4}$ nm × Time ($r^2 = 0.12$) for a 2.5-μm^2 area; for the detector initially exposed to acidic particles 141 nm in diameter (Figure 13), the regression equations are $2.7 + 3.8 \times 10^{-4}$ nm × Time ($r^2 = 7.3 \times 10^{-3}$) for a 100-μm^2 area and $0.14 + 1.9 \times 10^{-3}$ nm × Time ($r^2 = 0.4$) for a 2.5-μm^2 area. The slight increase in surface roughness over the 18-month period is insignificant with respect to the detector's performance as an acid monitor.

The dimensions of the acid sites on the two iron nanofilm detectors initially exposed to standard acidic particles are reported over 16 months of storage in Table 2. The reaction sites of 10 to 16 particles were sized each month. The diameters reported are full width at half maximum of the central peak of the ringed site. The results for the smaller-diameter standard suggested a possible increase in diameter of the central peak; however, the difference was not statistically significant. Different areas of the nanofilm were scanned each time. At the resolution used for these images, a single pixel represents 19.5 nm, which may be up to 30% of the central peak for the standard particles with 64-nm diameter. One pixel is less critical for the larger-diameter acid standard, and measures of the larger spots were clearly constant over time. When the diameter measurements were repeated on the stored images by measuring the larger total site diameter including the ring formation, it was clear that the sizes of the sites did not change.

Other parameters recorded for surface stability (not shown) were the count per 100 μm^2 of reaction sites with and without rings, the root mean square surface roughness, median height of the surface, and the bearing ratios at 95%

and 5%. The two bearing ratios indicate the slope of the cumulative frequency distribution of pixel heights. No meaningful differences were observed. Figure 14 shows a scan (2 μm × 2 μm) of the surface of a blank detector, with some of the measured parameters.

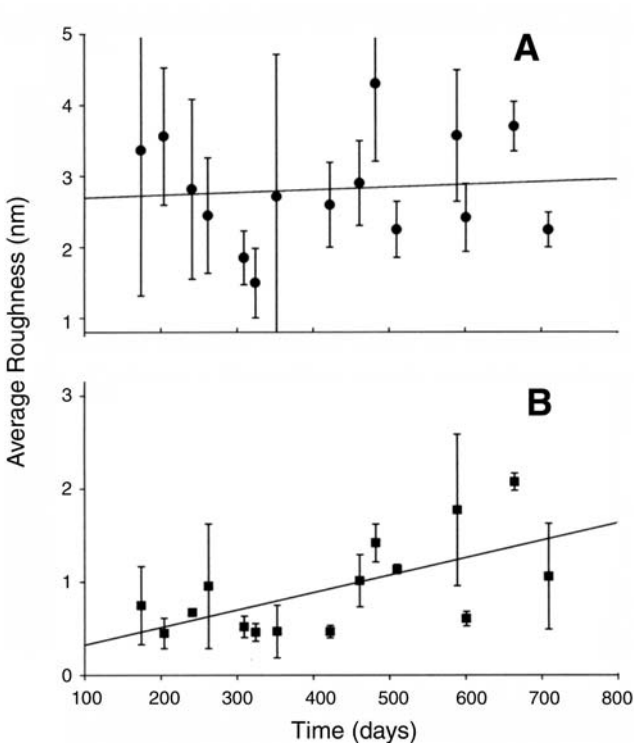

Figure 13. Average roughness over time of a quality control detector exposed to 141-nm acidic particles. ***A.*** Each point represents an average of four scanned areas (each of 100 μm^2), two in each of two quadrants. ***B.*** Zoomed scan area; each point represents an average of two scanned areas (each of roughly 2.5 μm^2), one in each of two quadrants. Vertical bars represent 1 SD of replicate roughness measurements.

Table 2. Heights and Diameters (means ± SD) of Reaction Sites on Two Acid-Exposed Detectors Stored Under Nitrogen at Room Temperature

Time (days)[a]	n[b]	Height (nm)	Diameter (nm)[c]	Outer Ring Diameter
Sample 141 nm				
174	14	39 ± 12	243 ± 68	498 ± 100
482	10	43 ± 9	279 ± 90	
504	16	44 ± 11	267 ± 55	524 ± 75
Sample 64 nm				
41	14	10.8 ± 1.6	74 ± 12	287 ± 68
464	12	6.9 ± 2.3	110 ± 10	
504	11	9.6 ± 2.2	134 ± 25	

[a] Elapsed time is days after exposure to 141-nm or 64-nm acidic particles.

[b] n is the number of reaction sites measured.

[c] Diameter is for the central (highest) peak.

Response to Humidity and Temperature

Visual observation of iron nanofilm detectors stored at high humidity (88% RH) and high temperature (39°C) showed that the surface of the detector with the highest number concentration of 141-nm H_2SO_4 particles started to corrode after 1 week and was completely destroyed in 2 weeks. The surfaces of the other detectors kept under these conditions for up to 3 months were partly corroded, and the remaining reaction sites were enlarged (Figures 6, 15). The detectors exposed to higher humidity (92% RH) at room temperature (22°C) showed some enlargement of sites, but the ring formation was still evident (Figure 16).

The roughness of the intact nanofilm surface changed, but not significantly, during exposure to high humidity at 22°C for most of the test detectors (Table 3). Changes were significant when the nanofilm was exposed to a more extreme temperature (39°C) and when there was a high density of acid reaction sites on the surface.

After 3 months of exposure to high humidity and temperature, sections of iron film released from the silicon support under the most extreme exposures, but surface parameters of the residual iron film did not change significantly. Thus count data were preserved for almost all of the test detectors, and even when portions of the surface began to release from the silicon support, data could be recovered from intact portions.

Table 3. Roughness of Detector Surfaces[a] Before and After 90-Day Exposure to High Humidity at 22°C and 39°C

Particle Size (nm)	Storage Conditions	Detector ID	Average Roughness ± SD (nm)			
			n[b]	Before Exposure	n	After Exposure
141	88% RH, 39°C	AA9	2	0.6 ± 0.20	4	15 ± 11
		FF4	3	0.8 ± 0.20	4	106 ± 37
64	88% RH, 39°C	II12	2	0.3 ± 0.20	4	42 ± 57
		CC15	2	0.2 ± 0.02	3	1.6 ± 0.50
		HH4	2	0.5 ± 0.10	2	0.8 ± 0.06
141	92% RH, 22°C	AA26	2	1.8 ± 0.07	2	2.5 ± 0.20
		BB15	2	1.8 ± 0.40	2	3.7 ± 0.80
64	92% RH, 22°C	HH12	2	0.3 ± 0.05	2	0.4 ± 0.20
		CC7	2	0.2 ± 0.06	2	1.0 ± 0.20
		GG7	2	0.8 ± 0.08	2	0.5 ± 0.20

[a] Particle-free area of the surface of detectors with previously deposited H_2SO_4 particles.

[b] n is the number of scans.

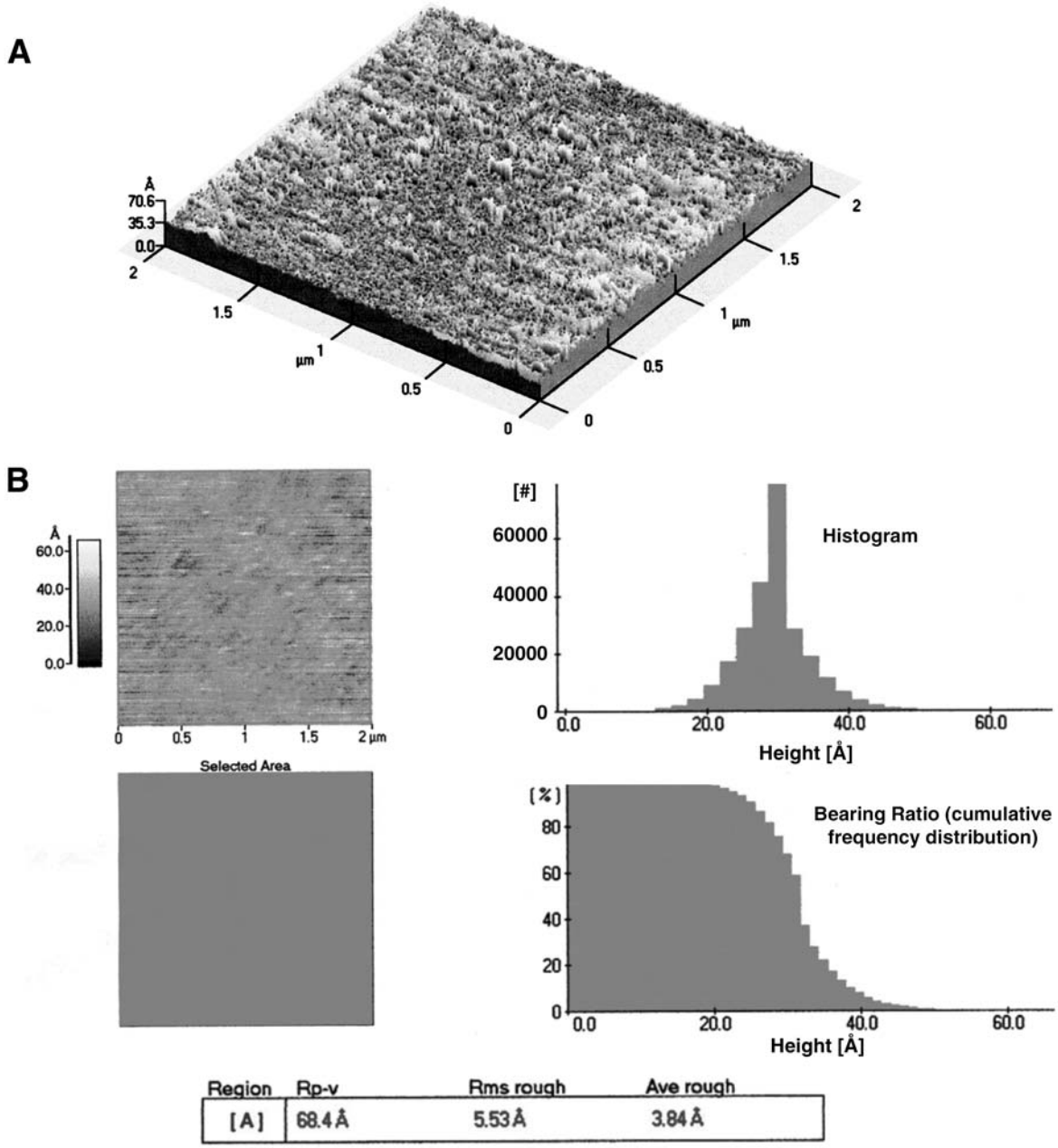

Figure 14. Blank iron nanofilm detector. ***A.*** Scan of a section (4 μm^2). ***B.*** Some of the parameters for a regional analysis of the scan provided by the AFM program. Rp-v = maximum peak to valley distance; Rms rough = root mean square roughness; Ave rough = average roughness.

Filtered Air Canisters

Twelve sets of blank detectors and detectors exposed to acid standards were placed in the filtered air canister and deployed in the field over the course of the study. These sets were thus exposed to varied weather conditions and, we assume, to varied concentrations of ambient pollutant gases. Occasionally slight damage was noted on some detectors by visual inspection after exposure. However, the intact surfaces on all of the preexposed detectors in the filtered air canisters were unchanged (Table 4. There was also no significant difference in the scans for either blanks (not shown) or acid-exposed standards (Figure 7). For most of the sampling sessions, standards preexposed to 141-nm particles were used, but three sets used standards with 64-nm particles. The largest potential discrepancy as determined visually was for the summer 1 sampling session; the

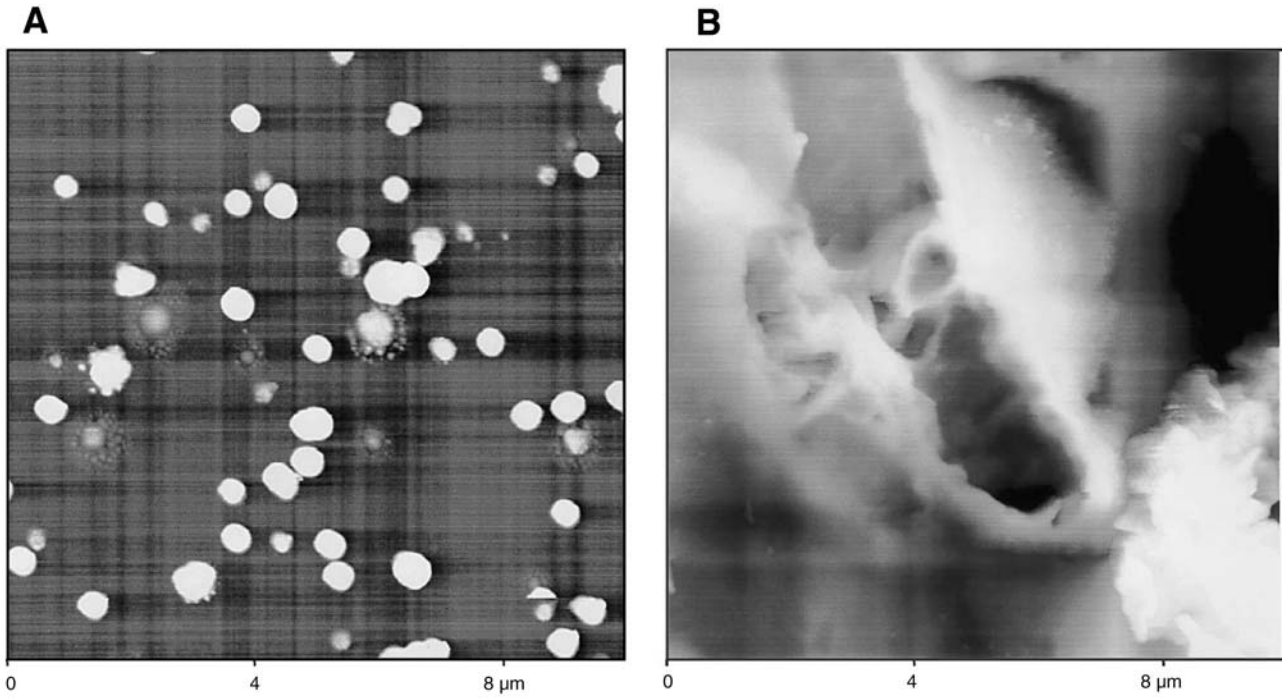

Figure 15. Iron nanofilm detector exposed to 141-nm H_2SO_4 particles. ***A.*** Image of a scan before storage. ***B.*** Scan of a different area of the same detector after storage for 3 months at 88% relative humidity and 39°C. As shown, sections of the iron-coated film did release from the silicon support at this extreme exposure, but surface parameters of the residual film did not change significantly.

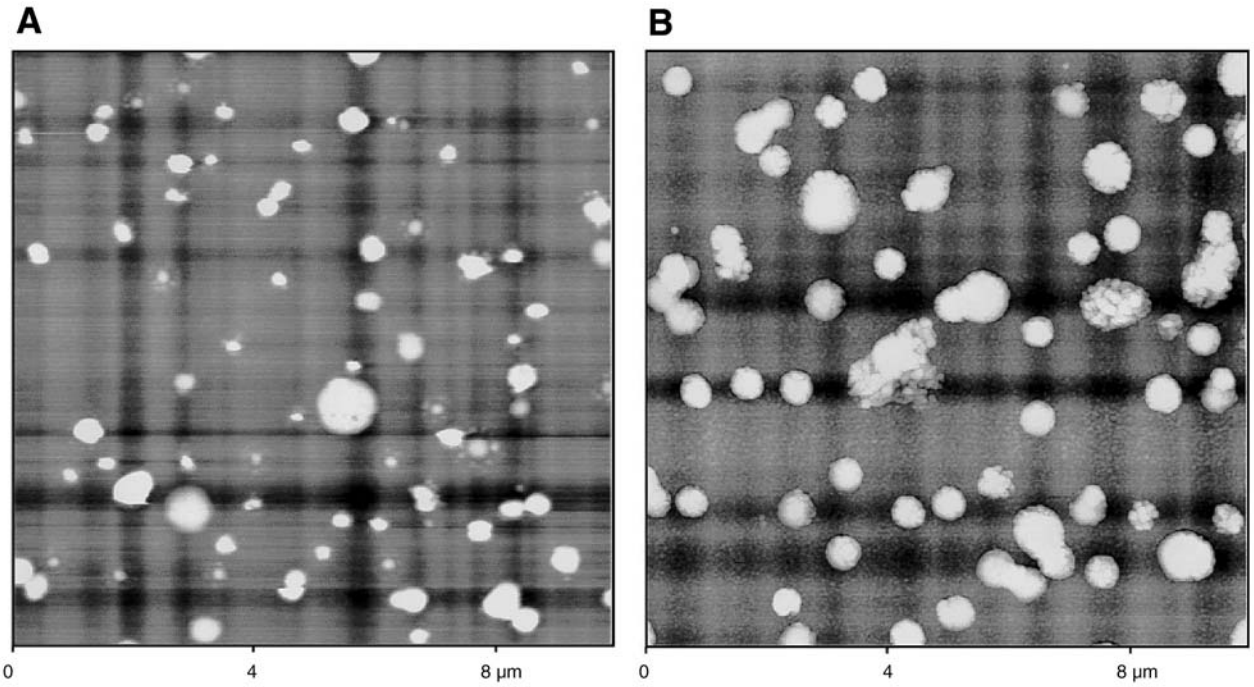

Figure 16. Iron nanofilm detector exposed to 141-nm H_2SO_4 particles. ***A.*** Image of a scan immediately before storage. ***B.*** Scan of a different area on the same detector after storage for 3 months at 92% relative humidity and 22°C.

reaction sites on the detectors preexposed to acid standard appeared slightly enlarged, but when measured their sizes compared closely to the measurements made immediately after the initial exposure to the acid standard (not shown). As previously noted, the ability to observe rings is subject to AFM scan settings, which are adjusted by the microscope for the heights of any material on the scanned surface.

MOI-EAS DETECTORS

Duplicate iron nanofilm detectors were deployed in the MOI-EAS for all sampling sessions to measure the average weekly number concentrations of total and acidic ultrafine particles. For the first field sampling session, six paired sets of detectors were deployed for time periods ranging from 2 to 7 days. We planned to remove and replace one set every 48 hours to avoid possible saturation of the detectors. Saturation in this context refers to overlap of particles that would complicate the analysis. The procedure ensured that at least two measurable sets would be available that could be averaged and interpreted to give the total number deposited during a 1-week sampling session.

To indicate the array of data recorded for the MOI-EAS samples, Table 5 presents the detailed counts on each of the pairs of detectors used in the first sampling session (summer 1: July 14 to July 21, 1999). The number concentrations of both total and acidic ambient particles less than 100 nm in diameter are shown in Table 6. These represent the mean number of particles per cm^3 of air over the number of days for which the detector was exposed. Detectors deployed for 2, 4, and 6 elapsed days beginning on July 14 had decreasing mean number concentrations of acidic particles despite the increasing number of sampling days. This implies that there was an episode of high acidity at the beginning (July 14 through 16) that declined over the next few days. The detectors that began sampling on July 16 showed lower mean concentrations of acidic particles over the last 5 and 3 days of the session than over the first 2 days. The total number concentration of ambient particles also was quite high during the first 2 days of sampling and declined during the later days; however, the fraction that was acidic remained quite high overall. The weather was very hot and humid during much of this session. Although the statistical errors were large, we obtained a convincing measure of the number concentration of these very small acidic particles in air.

There was no problem with saturation on any of the detectors deployed for the first sampling session, so only two detectors were deployed in subsequent sessions.

Table 7 presents the array of data, including surface roughness, from the replicate samples collected in the MOI-EAS for all of the outdoor sampling sessions. The

Table 4. Average Roughness of Blank and Acid-Exposed Detectors Subsequently Exposed to Ambient Gases[a] (mean ± SD)

Session and Sample	Average Roughness (nm)	
	Over 100 μm^2	Over Small Background Area (zoomed)[b]
Summer 1		
141 nm before	3.3 ± 0.59	0.80 ± 0.24
141 nm after	1.7 ± 0.23	0.48 ± 0.14
Blank before	0.44 ± 0.10	
Blank after	0.42 ± 0.18	
Summer 2		
141 nm before	1.9 ± 0.81	0.36 ± 0.17
141 nm after	1.1 ± 0.16	0.26 ± 0.09
Fall 1		
141 nm before	5.4 ± 0.92	1.07 ± 0.44
141 nm after	4.4 ± 3.12	0.59 ± 0.29
Fall 2+3		
64 nm before	1.0 ± 0.53	0.39 ± 0.08
64 nm after	0.8 ± 0.24	0.31 ± 0.09
Blank before	1.01 ± 0.75	
Blank after	0.72 ± 0.25	
Winter 1		
141 nm before	5.3 ± 0.83	0.79 ± 0.26
141 nm after	6.8 ± 1.64	1.44 ± 0.34
Winter 2		
141 nm before	2.7 ± 1.03	0.21 ± 0.03
141 nm after	3.2 ± 0.63	0.26 ± 0.06
Winter 3 (NYC)		
141 nm before	6.4 ± 1.62	1.32 ± 0.12
141 nm after	3.8 ± 0.65	1.75 ± 1.00
Blank before	0.41 ± 0.06	
Blank after	1.09 ± 0.16	
Winter 4 (NYC)		
64 nm before	1.1 ± 0.02	0.32 ± 0.01
64 nm after	0.8 ± 0.06	0.39 ± 0.07
Spring 1		
64 nm before	0.6 ± 0.16	0.17 ± 0.02
64 nm after	1.7 ± 0.19	1.29 ± 0.72
Spring 2		
141 nm before	3.6 ± 1.65	0.52 ± 0.18
141 nm after	4.4 ± 3.92	0.83 ± 0.42
Blank before	0.39 ± 0.11	
Blank after	0.41 ± 0.10	
NIEM cafeteria		
141 nm before	6.7 ± 2.24	0.71 ± 0.64
141 nm after	2.9 ± 0.23	0.92 ± 0.30
Newburgh residence		
141 nm before	3.8 ± 0.68	1.84 ± 0.58
141 nm after	5.4 ± 0.68	1.60 ± 0.13
Blank before	0.81 ± 0.57	
Blank after	1.61 ± 1.96	

[a] Detectors were exposed in filtered air canister.

[b] No zooms were done on blanks.

Table 5. MOI-EAS Detector Measurements for Summer 1 Sampling Session

Detector ID	Exposure Dates (1999)	Days of Exposure	Number of Precipitation Cycles	Number of Scans	Number of Reaction Spots			
					Total	Per 100 μm^2 (mean ± SD)	Total with Rings	With Rings per 100 μm^2 (mean ± SD)
AA-22	07/14–07/21	7	149,969	16	694	43.4 ± 7.0	564	35.3 ± 5.7
CC-30	07/14–07/21	7	149,969	16	785	49.1 ± 8.1	688	43.0 ± 5.9
BB-33	07/14–07/20	6	129,789	16	636	42.4 ± 4.3	501	33.4 ± 4.7
HH-18	07/14–07/20	6	129,789	16	608	40.5 ± 9.2	508	33.9 ± 9.3
EE-11	07/14–07/18	4	85,789	16	658	44.3 ± 5.4	554	37.4 ± 6.0
EE-22	07/14–07/18	4	85,789	16	696	43.5 ± 8.5	556	34.8 ± 8.2
BB-32	07/14–07/16	2	43,304	16	695	43.4 ± 9.7	522	32.6 ± 8.5
EE-4	07/14–07/16	2	43,304	16	640	40.0 ± 5.8	494	30.9 ± 7.7
GG-16	07/16–07/21	5	106,665	8	349	43.6 ± 6.5	276	34.5 ± 10.6
CC-27	07/16–07/21	5	106,665	8	406	50.8 ± 10.9	222	27.8 ± 10.5
GG-6	07/18–07/21	3	64,180	7	200	28.6 ± 9.4	45	6.4 ± 2.3
FF-14	07/18–07/21	3	64,180	8	188	23.5 ± 4.8	92	11.5 ± 4.7

Table 6. Number Concentration of Total and Acidic Ultrafine Particles in Air Measured by MOI-EAS Detectors in Summer 1 (1999)

Detector IDs	Exposure Dates	Days of Sampling	Particles per cm^3 (mean ± SD)		
			Total *N*	Acidic *N*	Acidic (%)
AA-22, CC-30	07/14–07/21	7	621 ± 57	550 ± 77	88
BB-33, HH-18	07/14–07/20	6	599 ± 20	512 ± 5	86
EE-11, EE-22	07/14–07/18	4	990 ± 41	852 ± 2	86
BB-32, EE-4	07/14–07/16	2	1933 ± 118	1545 ± 60	80
GG-16, CC-27	07/16–07/21	5	893 ± 100	615 ± 94	69
GG-6, FF-14	07/18–07/21	3	789 ± 118	294 ± 118	37

roughness values indicate that the surface integrity of the iron nanofilm detectors was not impaired by exposure to the atmosphere or by the electric field applied by the EAS.

The mean number concentrations of ambient nonacidic, acidic, and total ultrafine particles measured for the outdoor sampling sessions are shown in Table 8. The number concentrations averaged over the period for each sampling session ranged from $(5 \pm 2) \times 10^2/cm^3$ to $(28 \pm 14) \times 10^2/cm^3$ for total particles, from $(1.0 \pm 0.9) \times 10^2/cm^3$ to $(7 \pm 2) \times 10^2/cm^3$ for acidic particles, and from $(0.8 \pm 0.2) \times 10^2/cm^3$ to $(25 \pm 12) \times 10^2/cm^3$ for nonacidic particles.

UDM DETECTORS

The initial field tests revealed that very few particles were collected on the iron nanofilm detectors placed at the second and third locations in the UDMs. This resulted from a combination of low deposition efficiency and too few ambient particles in the size range to provide adequate samples at these locations within the UDMs. (The decrease in deposition efficiency with increased channel length is not linear, as seen from equation [3]; it decreases as the particle diameter increases, but it is not the same at all detector locations.) Results given here are from scans of the duplicate detectors closest to the inlet. Since few reaction spots larger than 100 nm were observed on the detectors, a geometric mean of theoretical deposition efficiency values for 30-nm and 100-nm particles was used to calculate airborne concentrations. The calculated mean deposition efficiencies for the summer sampling sessions were marginally higher owing to lower flow rates. These values

Table 7. MOI-EAS Detector Measurements for All Outdoor Sampling Sessions

Detector ID	Sampling Session	Dates	Days of Exposure	Number of Precipitation Cycles	Number of Scans	Number of Reaction Spots				Roughness at Zoom (nm) (mean ± SD)
						Total	Per 100 μm^2 (mean ± SD)	Total with Rings	With Rings per 100 μm^2 (mean ± SD)	
AA-22	Summer 1	07/14–07/21/1999	7	149,969	16	694	43.4 ± 7.0	564	35.3 ± 5.7	0.28 ± 0.04
CC-30		07/14–07/21/1999	7	149,969	16	785	49.1 ± 8.1	688	43.0 ± 5.9	0.22 ± 0.08
HH-3	Summer 2	07/21–07/28/1999	7	148,873	8	175	29.2 ± 5.9	144	24.0 ± 5.4	0.32 ± 0.13
CC-31		07/21–07/28/1999	7	148,873	4	269	67.3 ± 16.9	41	10.3 ± 3.6	0.51 ± 0.14
HH-6	Fall 1	10/21–10/28/1999	7	149,988	5	422	84.4 ± 9.2	50	10.0 ± 2.0	0.19 ± 0.07
AA-35		10/21–10/28/1999	7	149,988	4	289	72.3 ± 10.4	26	6.5 ± 2.9	0.74 ± 0.37
AA-12	Fall 2+3	10/28–11/11/1999	14	289,632	4	804	201.0 ± 30.1	148	37.0 ± 7.5	0.47 ± 0.02
II-8		10/28–11/11/1999	14	289,632	4	388	97.0 ± 19.1	32	8.0 ± 7.0	1.45 ± 0.47
GG-15	Winter 1	02/01–02/08/2000	7	149,603	4	290	72.5 ± 6.2	163	40.8 ± 5.3	0.85 ± 0.21
EE-33		02/01–02/08/2000	7	149,603	4	314	78.5 ± 1.3	230	57.5 ± 4.6	1.58 ± 0.10
DD-1	Winter 2	02/08–02/16/2000	8	172,841	4	231	57.8 ± 2.5	136	34.0 ± 2.2	0.57 ± 0.09
CC-5		02/08–02/16/2000	8	172,841	4	339	84.8 ± 13.2	230	57.5 ± 10.3	0.50 ± 0.35
DD-11	Winter 3	03/09–03/16/2000	7	146,460	4	440	110.0 ± 41.7	77	19.3 ± 9.7	0.40 ± 0.10
EE-5	(NYC)	03/09–03/16/2000	7	146,460	4	660	165.0 ± 12.6	18	4.5 ± 4.7	1.87 ± 0.99
FF-19	Winter 4	03/16–03/23/2000	7	147,200	4	1059	264.8 ± 20.8	131	32.8 ± 10.9	2.00 ± 0.48
DD-17	(NYC)	03/16–03/23/2000	7	147,200	4	501	125.5 ± 13.8	37	9.3 ± 3.1	1.47 ± 0.73
AA-33	Spring 1	05/01–05/08/2000	7	151,001	4	113	28.3 ± 5.9	10	2.5 ± 1.7	0.86 ± 0.32
CC-12		05/01–05/08/2000	7	151,001	4	199	49.8 ± 6.9	47	11.8 ± 3.1	2.00 ± 1.40
EE-35	Spring 2	05/08–05/15/2000	7	151,880	4	167	41.8 ± 7.7	44	11.0 ± 3.4	1.84 ± 1.40
BB-23		05/08–05/15/2000	7	151,880	4	198	49.5 ± 14.6	66	16.5 ± 2.4	1.45 ± 1.18

are shown in Table 9, which presents the resulting number concentrations of acidic and total particles during each sampling session.

The results for the UDM with the low flow rate were variable. The sampling time was too short for the low concentrations observed in Tuxedo. The winter 3 and 4 sampling sessions in New York City seemed to provide better data as the number concentration was about 10 times higher.

The number concentrations for the UDM operated at the higher flow rate were comparable to the concentrations calculated from the SMPS measurements, except for the winter sampling in New York City (see Table 10). The iron nanofilm detectors used during the winter may have been overloaded.

Table 8. Number Concentration of Acidic and Nonacidic Ultrafine Particles in Air Measured by MOI-EAS Detectors

Sampling Session	Number of Particles per cm^3 (mean ± SD)		
	Nonacidic	Acidic	Total
Summer 1	72 ± 20	550 ± 77	621 ± 57
Summer 2	403 ± 532	200 ± 78	603 ± 454
Fall 1	956 ± 86	116 ± 35	1072 ± 121
Fall 2+3	906 ± 386	164 ± 149	1070 ± 535
Winter 1	343 ± 107	692 ± 167	1035 ± 60
Winter 2	287 ± 30	558 ± 203	844 ± 233
Winter 3 (NYC)	1779 ± 710	171 ± 150	1950 ± 560
Winter 4 (NYC)	2462 ± 1174	301 ± 238	2763 ± 1412
Spring 1	417 ± 121	99 ± 91	516 ± 212
Spring 2	415 ± 22	191 ± 54	605 ± 76

Measurements in the NIEM cafeteria at Tuxedo and outdoors near the window indicated that the particle number concentration was almost twice as high indoors (7000 ± 5000/cm^3) as compared with outdoors (3100 ± 560/cm^3). There were 3 times as many acidic particles indoors (1400 ± 800/cm^3) as compared with outdoors (460 ± 180/cm^3).

Indoor measurements at the residence in Newburgh indicated a total average particle concentration of approximately 6700 ± 3100/cm^3 and an average acidic particle concentration of 170 ± 240/cm^3. Because the pumps failed sporadically, we did not include outdoor measurements from the Newburgh residence in the analyses; however, the total number of particles deposited was about two thirds as many as were deposited on the indoor detectors, and no acidic sites were observed on the outdoor detectors.

MOI FILTERS

The size distributions of H^+, SO_4^{2-}, and NH_4^+ for the size-fractionated samples obtained during each outdoor sampling session using the MOI are shown in Figure 17. Each impactor stage collects particles within a given size range. The final filter collects particles that penetrate the last stage (< 88 nm). The size distribution results are presented for the midpoint diameter of that size range. The highest ambient H^+, SO_4^{2-}, and NH_4^+ concentrations were measured in the size range between 280 and 530 nm. The distributions also suggest that another small peak of these ions existed in the size range below 88 nm. Although the total ion concentrations for the same midpoint diameter varied from one sampling session to another, the distribution profile was the same overall.

Table 9. Number Concentration (mean ± SD) of Ultrafine Particles in Air Measured with UDMs at Two Flow Rates

Sampling Session	Days	E_f (10^{-9})[a]	Particles per cm^3 at 10 cm^3/min		E_f (10^{-10})[a]	Particles per cm^3 at 200 cm^3/min	
			Total	Acidic		Total	Acidic
Summer 1	7	7.3	16,800 ± 9100	40 ± 60			
Summer 2	7	7.5	6400 ± 6100	180 ± 260			
Fall 1	7	7.1	7400 ± 500	530 ± 750			
Fall 2+3	14	7.1	4800 ± 130	1100 ± 370			
Winter 1+2	14	7.1	4800 ± 350	970 ± 230			
Winter 2	7				7.7	3600 ± 2200	70 ± 100
Winter 3+4 (NYC)	14	7.1	7100 ± 70	1800 ± 200	7.7	22,200 ± 5600	720 ± 20
Spring 1+2	14	7.1	7300 ± 4000	260 ± 370	7.7	3900 ± 840	510 ± 240

[a] E_f is efficiency of particle deposition, given per scan area.

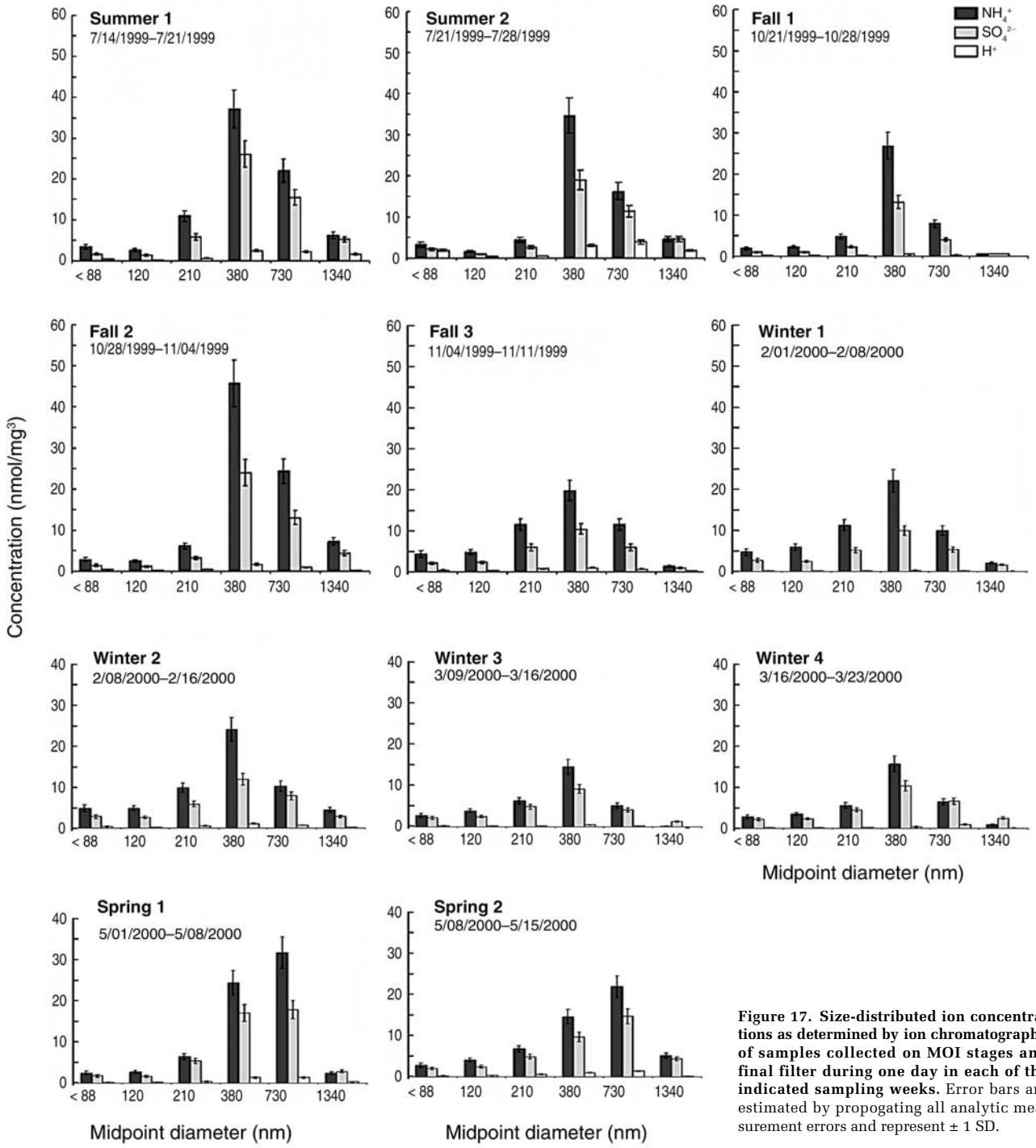

Figure 17. Size-distributed ion concentrations as determined by ion chromatography of samples collected on MOI stages and final filter during one day in each of the indicated sampling weeks. Error bars are estimated by propogating all analytic measurement errors and represent ± 1 SD.

Average ion concentrations over all sampling sessions are shown in Figure 18. Most of the sulfate appeared to be in the form of $(NH_4)_2SO_4$; however, there was a small but consistent excess of SO_4^{2-}. The H^+/SO_4^{2-} ratio is shown as a function of particle size (midpoint diameter) in Figure 19. The somewhat higher ratio for the smallest size range suggests greater excess acidity for these very small particles.

The ambient concentration of H^+ in the smallest size range is shown in Figure 20; the fall 2 and fall 3 data are combined because the particle count samples were for this 2-week period. The total number concentrations of acidic particles calculated from the MOI-EAS iron nanofilm detectors for these periods are shown in Figure 21 for comparison with the total H^+ concentrations.

SMPS DATA

The recorded particle size spectra from the SMPS were averages of three scans obtained every 30 minutes. The distribution varied considerably during a single day, as illustrated by Figure 22. The average particle size distribution for the same day is presented in Figure 23.

In the Tuxedo samples the individual particle size spectra, within the measured range of 10 to 300 nm, were frequently bimodal; the first peak was at 10 to 50 nm, and the second was at 70 to 200 nm. Unimodal spectra were mostly found at night with peaks at 50 to 200 nm. Trimodal spectra were also found occasionally with peaks at about 15, 50, and 150 nm. Aitken mode particles (20 to 80 nm) were often found in early morning and late afternoon. Low particle number concentrations were often found with southerly winds.

In New York City the individual particle size spectra were usually unimodal with maximum particle size below 50 nm.

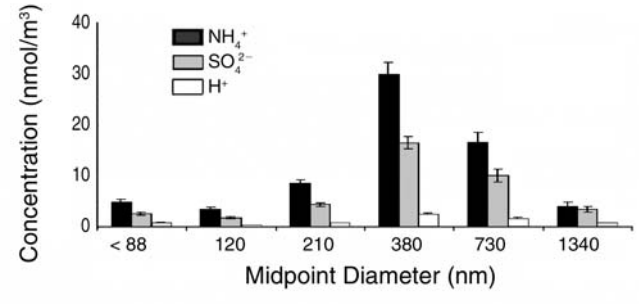

Figure 18. Size-distributed ion concentrations of samples collected on MOI stages and final filter averaged across the 11 days. Error bars represent ± 1 SD.

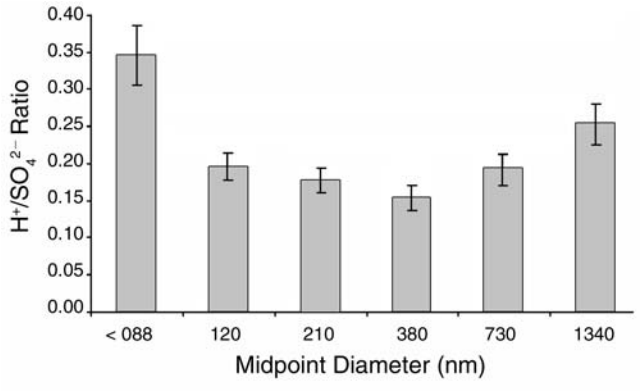

Figure 19. H^+/SO_4^{2-} ratio as a function of particle size (midpoint diameter) of samples collected on MOI stages and final filter averaged across the 11 sampling session days. The results suggest greater excess acidity for very small particles. Error bars represent ± 1 SD.

The average size spectra for the first sampling week of each season in Tuxedo are shown in Figure 24. Those for the winter 1 session in Tuxedo and the winter 3 session in New York City are shown in Figure 25. The particle concentrations were lower for summer and fall, and in fall and spring the distributions were often unimodal with the maxima occurring in smaller particles.

Very high number concentrations of particles smaller than 20 nm were found in the fall, as compared with the summer sampling sessions. This was most likely due to the eight nucleation events that occurred during the fall sessions (a nucleation event is illustrated in Figure 26). Overall, no nucleation events were observed in summer, eight in fall, one in winter, and five in spring. They occurred

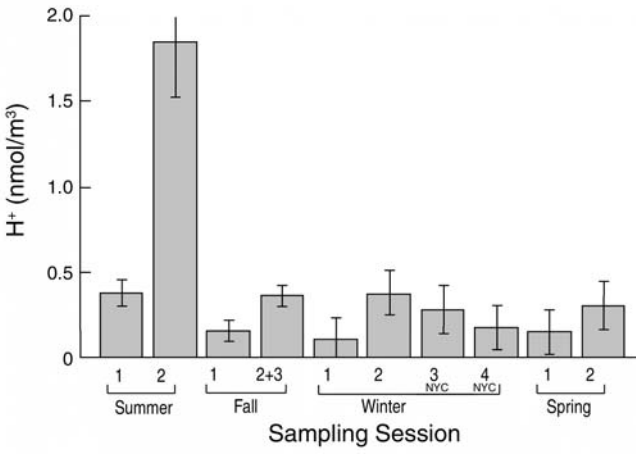

Figure 20. Mean ambient concentration of H^+ in particles smaller than 100 nm collected on the polycarbonate filter after the MOI for one day in each sampling session. Error bars are estimated by propogating all analytic measurement errors. Error bars represent ± 1 SD.

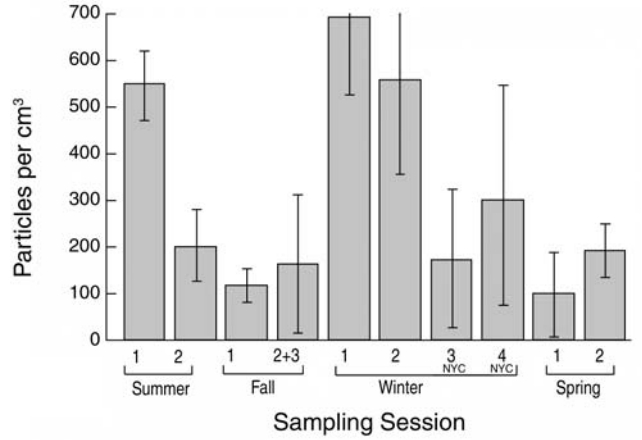

Figure 21. Number concentration of acidic particles smaller than 100 nm collected on the MOI-EAS detectors for each sampling session day. Error bars represent ± 1 SD.

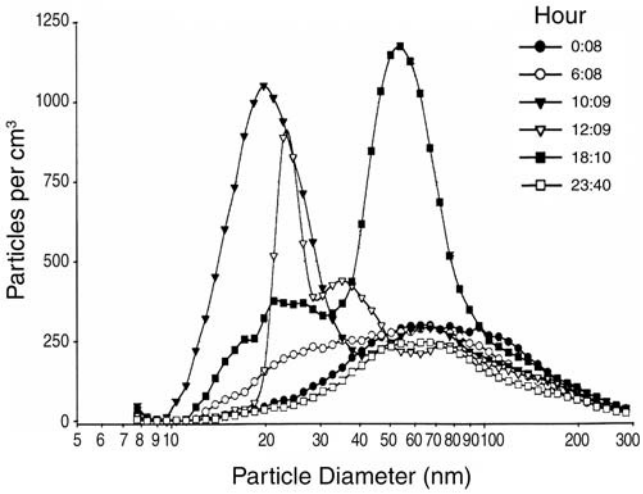

Figure 22. Number-weighted particle size distribution spectra obtained from the SMPS at approximately 4-hour intervals during 24 hours in the summer 1 sampling session. Data are for July 20, 1999, in Tuxedo. Each distribution is the average of three scans.

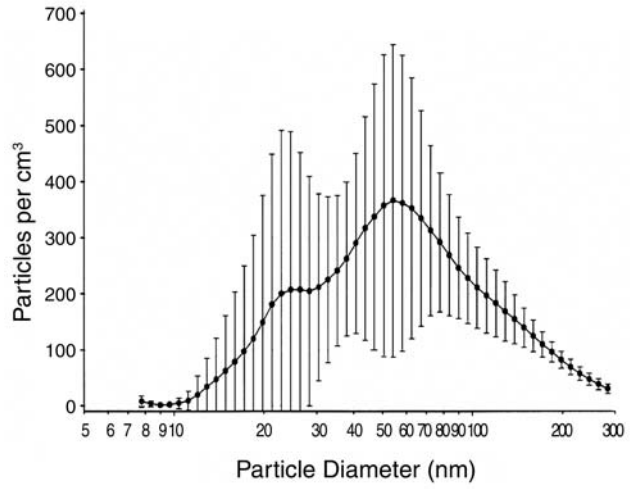

Figure 23. Average particle size distribution from the SMPS for the same day as in Figure 22. Each point is the mean ± 1 SD of 48 measurements from scans taken at 30-minute intervals. Three consecutive scans were averaged to obtain one measurement.

mainly in early afternoon with sustained westerly or southwesterly winds. The particle number concentration during these events increased from 10 to 100 fold.

CNC DATA

An example of the continuous data observed with the CNC for the number concentration of particles is shown as hourly averages for the summer 1 and summer 2 sampling sessions in Figure 27. The hourly averages were visually estimated from the chart-recorded data. Because the particle size distribution was not known at each time point, these

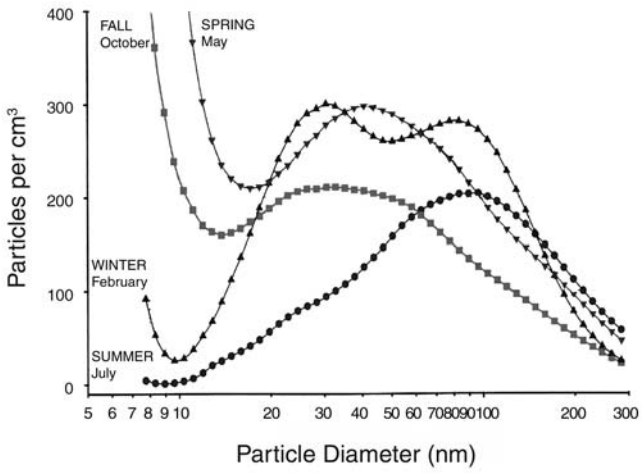

Figure 24. Average particle size spectra from the SMPS for the first week of each sampling session in Tuxedo. Each point represents an average of over 300 spectra taken at 30-minute intervals.

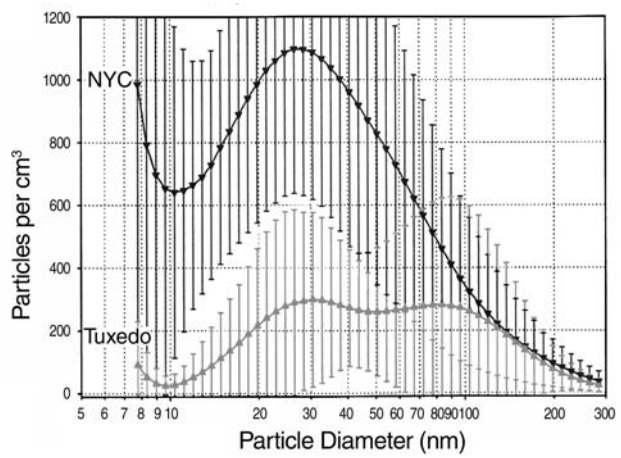

Figure 25. Average particle size spectra from the SMPS for the winter 1 sampling session in Tuxedo and the winter 3 session in New York City. Each point represents an average of over 300 points from scans taken at 30-minute intervals.

values could not be corrected for penetration efficiency through the sample inlet tubing. The overall penetration efficiency was roughly 90%, so the actual values would be higher than those shown in Figure 27.

At the Tuxedo site, the total number concentration of particles was usually between 2000 and 15,000/cm^3, but ranged from a few hundred to over 100,000/cm^3 for short-duration peaks. Averages at the New York City site were generally about 10 times greater than those at Tuxedo.

To compare the CNC and SMPS data, the latter were corrected by the ratio between the penetration efficiencies of the sampling lines for the two instruments. Comparative measurements are shown in Figure 28 for a single winter day in Tuxedo and a similar day in New York City. For the

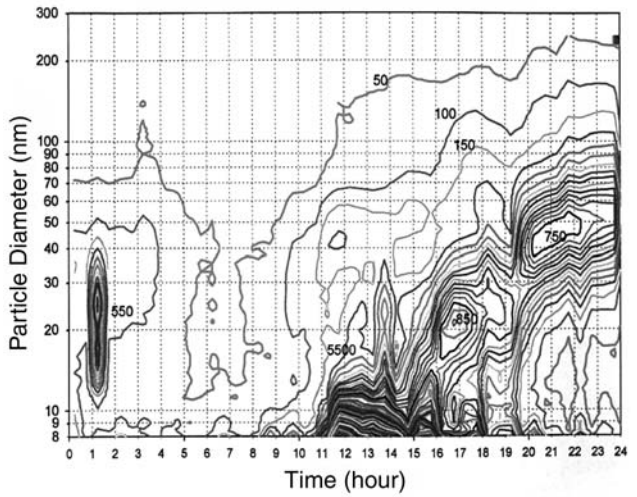

Figure 26. Evolution of size distribution during a single day in the fall 1 session. The nucleation event shows development of a high concentration of particles less than 10 nm in diameter. The contours are lines of equal number concentration in particles per cubic centimeter. The interval between contours is 50 particles/cm^3. Data are for October 25, 1999, in Tuxedo.

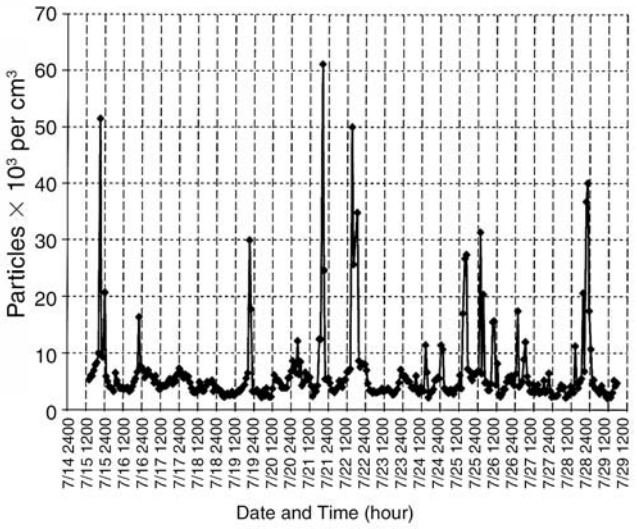

Figure 27. Particle number concentrations as measured by CNC and shown as 1-hour averages for the summer 1 and summer 2 sampling sessions in Tuxedo.

most part the CNC measurements showed reasonable correspondence with the total calculated from the SMPS. Agreement was at times very good, but spikes recorded by either one of the instruments were not always seen by the other.

Measurements taken indoors at the NIEM cafeteria were similar to typical outdoor values except for peaks during the weekday lunch hours (Figure 29). The average count estimated from Figure 29 is similar to the value of approximately 7000 particles/cm^3 estimated from the UDM detector samples.

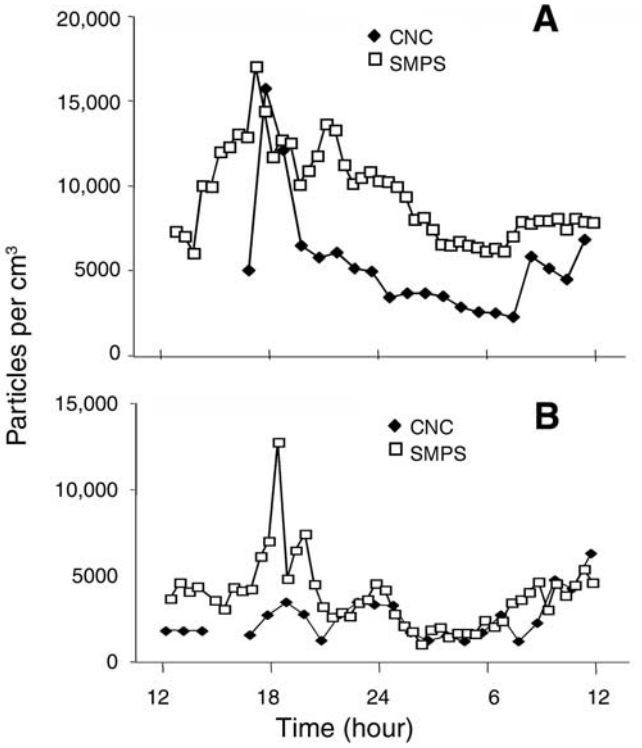

Figure 28. Particle number concentrations measured by CNC (1-hour averages) and SMPS (average of 3 scans taken over a 30-minute interval) during winter sampling sessions. ***A.*** Tuxedo, February 10 to 11, 2000. ***B.*** New York City, March 16 to 17, 2000. Agreement between CNC and SMPS data was generally good, but spikes recorded by either of the instruments were not always identified by the other.

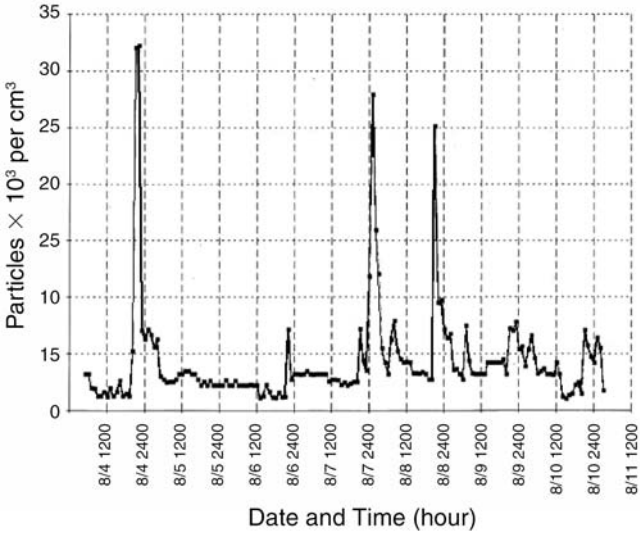

Figure 29. Particle number concentrations measured by CNC (1-hour averages) indoors at the NIEM cafeteria. Note peaks during the weekday lunch hour on Friday (8/4/2000), Monday, and Tuesday, and smaller increases on Wednesday and Thursday.

DISCUSSION

We used iron nanofilm detectors to determine the number concentration of strongly acidic ambient ultrafine particles. The quality control work carried out in these experiments established that the detectors could be used with confidence under a range of ambient conditions, particularly in temperate climates. Under extreme conditions of high humidity and high temperature, the surface film sometimes detached from the support, but any remaining portions of the film still produced reliable data.

Exposure of the iron nanofilm detectors to ambient gases in a filtered air canister during the field tests had no effect on the nanofilm quality as determined by observation and by surface parameters measured on AFM scans after the field deployment. We did not, however, measure concurrent concentrations of ambient gases. It is possible that high concentrations of some gases would affect the surface. For example, if ozone was very low during our experiments, it may have been depleted by the setup. So, damage from ozone should be considered in future sampling.

Furthermore, high concentrations of reactive gases might alter already formed reaction sites. After some of the nanofilms with reaction sites were deployed in the filtered air canister, we noted subtle differences, which we attributed to small unavoidable variations in setting of the AFM scan parameters. The possibility, however, that there was some real effect deserves further exploration.

It would also be of interest to determine the reaction rate of the acid site formation and explore whether subtle differences in reaction sites could be detected as a function of particle acidity. We used a dichotomous approach in which we considered a ringed reaction site to represent an acidic particle, and any other site a nonacidic particle. This was a pragmatic choice when setting the protocol for counting relatively large numbers of field samples. Further study may offer the opportunity to obtain more information on the distribution of acid in individual particles.

Particles can be deposited onto the iron nanofilm detectors either by precipitation using electrical or thermophoretic methods, or by simply drawing air through a channel and allowing particles to deposit by diffusion (eg, as in our new UDM). Initially, we considered using prefiltration with a sieving-type (eg, Nucleopore) filter to remove large particles when sampling and applying corrections for the loss of small particles. However, the number of larger particles is so low compared with the number of ultrafine particles that prefiltration is not really necessary. Comparatively few large particles precipitated onto the detectors either electrically or by gravitational settling. Further, at the flow rates used in our UDM, the deposition efficiency of most particles in the accumulation mode was quite low, so that, in practice, the collected particles represented the fraction with the smallest diameters we could visualize. Finally, an optical image is always used to select the areas to be scanned by AFM, so any large particles visible on the optical image are easily avoided.

The EAS we used was very effective. For these experiments the flow rates and operation of the device were checked twice daily; however, the reliability of the instrument suggests that it could be deployed for much longer time periods without concern. In the experiments reported here that used the MOI-EAS system, we preselected particles with diameters less than 100 nm. If preselection is not done, the deposited particles and reaction sites could be individually sized to derive the size distributions of total particles and acidic particles. Our previous work showed that the reaction sites were larger than the original particles, and calibration was required to determine the original particle size. However, analysis for particle size is labor intensive and time consuming. For this report we simply counted all observed particles.

One practical test of the agreement in the number concentrations measured by different systems was to compare the ambient particle concentrations measured using the SMPS with those calculated from particles counted on the iron nanofilm detectors exposed in the MOI-EAS and the UDMs. Only particles that penetrated the seventh stage of the MOI (diameter less than 100 nm) were transmitted to the EAS, and only particles larger than about 35 nm are reliably detected by AFM, so the relevant comparison was with the SMPS measurements averaged for particles from 35 to 100 nm. These are shown (averaged over the duration of each sampling session) in Figure 30. The ambient particle

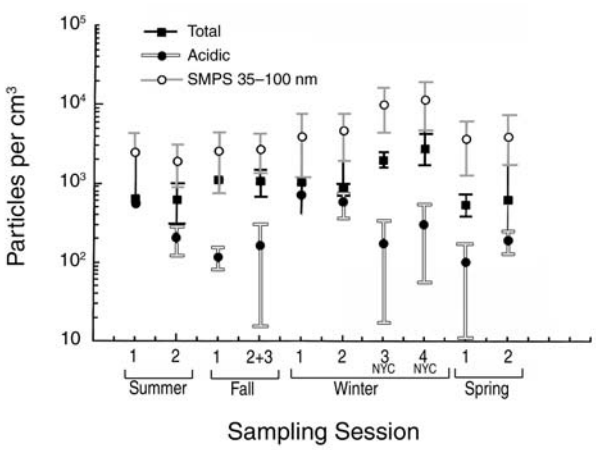

Figure 30. Comparison among the total and acidic number concentrations counted on detectors exposed in the MOI-EAS (Table 8) and total 35 to 100 nm concentrations measured with the SMPS. For SMPS, hundreds of points were averaged, but the concentrations were variable over the course of a day as shown on prior figures. Error bars represent ± 1 SD.

concentrations were temporally quite variable (eg, see Figures 23 and 25), and this was reflected in large standard deviations in the calculated SMPS averages. For the UDM concentrations the relevant comparison was with the SMPS measurements averaged for particles from 40 to 300 nm (Table 10).

Figure 30 also shows the number concentrations of particles that were acidic, as determined from the number of ringed reaction sites on the MOI-EAS iron nanofilm detectors for each sampling session. The percentage of particles that were acidic over the sampling session is shown in Figure 31.

From the data presented in Figure 30, it appears that the measurements by AFM analysis of the detectors placed in the MOI-EAS (Table 8) underestimated the total number concentrations when compared with- the SMPS measurements. It is logical to assume that the number of acidic particles was also underestimated. This problem most likely resulted from both the quality of the AFM tips and the setting and interpretation of the imaging parameters. Moreover, the elevated rings around acidic particles are sometimes difficult to recognize. Continuing improvements in imaging software will ultimately provide better tools for differentiating the particles and reaction sites.

The number concentrations of acidic particles measured by the MOI-EAS and UDM detectors also were compared (Table 11). The mean values for some of the measurements showed remarkably good agreement, but the standard deviations were large. For the UDMs a large part of the uncertainty was attributable to the relatively low number of counts obtained during some of the sampling sessions. As noted previously, we assumed a Poisson distribution for the counts, which resulted in large relative error estimates for low numbers. These measurements provide the first estimates of the concentration of acidic ultrafine particles. Integrated sampling over longer time periods can provide more precise measurements.

Comparative measurements revealed a lack of correspondence between the acidic content of ultrafine particles and the number concentration of acidic ultrafine particles, as determined from the MOI-EAS measurements

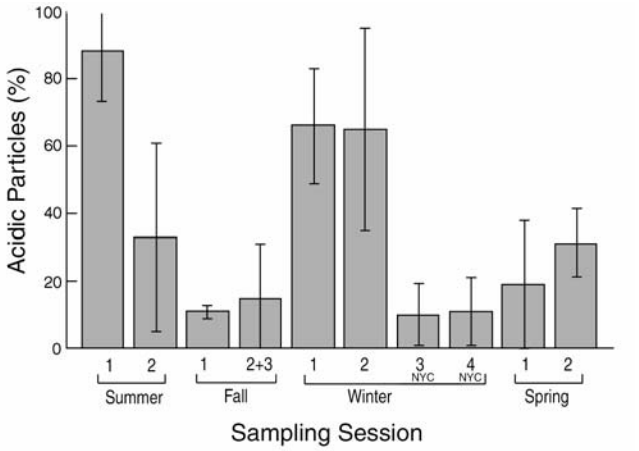

Figure 31. Percentage of total ultrafine number concentration represented by acidic ultrafine particles (as determined from ringed reaction sites) on MOI-EAS detectors for each sampling session. The data used to plot Figure 30 were also used to calculate the percentages here. Error estimates were propagated from SDs in Table 8.

Table 10. Number Concentration of Ultrafine Particles in Air Measured with SMPS and UDMs at Two Flow Rates

Sampling Session	Days of Exposure	Particles per cm^3 (mean ± SD)		
		SMPS[a]	UDM at 10 cm^3/min	UDM at 200 cm^3/min
Summer 1	7	4313 ± 2306	16,800 ± 9100	
Summer 2	7	2999 ± 1537	6400 ± 6100	
Fall 1	7	3296 ± 2246	7400 ± 500	
Fall 2+3	14	4043 ± 2357	4800 ± 130	
Winter 1	7			3600 ± 2200
Winter 2	7	6332 ± 3446		
Winter 1+2	14	5917 ± 4451	4800 ± 350	
Winter 3+4 (NYC)	14	11,405 ± 7038	7100 ± 70	22,200 ± 5600
Spring 1+2	14	5137 ± 3285	7300 ± 4000	3900 ± 840

[a] Particles with diameter from 40 to 300 nm were used for comparison with UDM measures.

Table 11. Number Concentration of Acidic Ultrafine Particles in Air Measured by UDM and MOI-EAS Detectors

Sampling Session	Days of Exposure	Number of Acidic Particles per cm^3 (mean ± SD)		
		UDM at 10 cm^3/min	UDM at 200 cm^3/min	MOI-EAS
Summer 1	7	40 ± 60		550 ± 77
Summer 2	7	180 ± 260		200 ± 78
Fall 1	7	530 ± 750		116 ± 35
Fall 2+3	14	1100 ± 370		164 ± 149
Winter 1	7			692 ± 167
Winter 2	7		70 ± 100	558 ± 203
Winter 1+2	14	970 ± 230		
Winter 3 (NYC)	7			171 ± 150
Winter 4 (NYC)	7			301 ± 238
Winter 3+4 (NYC)	14	1800 ± 200	720 ± 20	
Spring 1	7			99 ± 91
Spring 2	7			191 ± 54
Spring 1+2	14	260 ± 370	510 ± 240	

(Figures 20 and 21). A single particle of 100-nm diameter may contain the same acid volume as many smaller particles if the particles are pure acid droplets. However, if the acid is coated on the surface of a small particle, as is likely, then the relation of number to mass is more complex. This relation could be examined more easily with larger particles, although the portion of the particle that is acidic may vary with particle size. As shown in Figure 17, most of the strongly acidic mass was found in particles with diameters between 280 and 530 nm. Particles of this size are visible with optical microscopy and thus could be easily studied using iron nanofilms on glass slides.

Given the statistical variability in the number of particle counts and the errors in diameter measurement introduced by current AFM technology (eg, the AFM tip and the resolution of the images), the lack of correspondence in our data is not surprising. Of course, it would be possible to produce images with much better resolution by using much smaller scan areas; however, the tradeoffs would be fewer particles counted per scan and substantial increases in the analytical time required.

The simplicity of the UDM system allowed us to begin integrated air sampling for total and acidic ultrafine particles soon after the World Trade Center disaster on September 11, 2001. Because of the fires, which continued to burn until December 20, 2001, it was important to document this particle size fraction, and no other simple samplers were available for this monitoring. We deployed several UDMs containing both iron nanofilm detectors and bare silicon detectors at the Mt Sinai–NYU Downtown Hospital, a few blocks from what has come to be known as ground zero. The UDMs were in place from September 19 through 25, 2001. We also deployed both types of detectors in the MOI-EAS from September 28 to December 20, 2001.

In the future these detectors will allow monitoring of acidic particles during epidemiologic studies of the health effects of ambient particles such as those carried out in Erfurt, Germany (Peters et al 1997b; Wichmann and Peters 2000). The approach used to detect acidic ultrafine particles by reaction sites on iron-coated nanofilms can be extended to characterize other kinds of ambient particles by use of thin films coated with different organic materials. We have tested a variety of materials that develop reaction sites when exposed to specific components of the ambient aerosol. Further development may ultimately allow deployment of sets of detectors with coatings that identify several classes of chemical compounds (Cohen et al 2002). Improvements in particle-charging technology that are becoming available will allow much more efficient electrical precipitation of particles onto the detectors. That should provide good short-term sampling results. Currently, use of these detectors is limited by the time required for scanning the nanofilm and counting reaction sites. One or more atomic force microscopes is required, along with an experienced operator to set scan parameters, confirm the surface integrity, and view and count the particle images.

In the work reported here, only one or two detectors per day could be analyzed. The need for frequent checks of the system with quality control samples (eg, standards) further limits the speed of sample throughput. As with most new devices, technological improvements continue to be forthcoming. An automatic scanning system using improved atomic force microscopes, together with automated sample-handling systems, may ultimately permit high throughput of samples. However, use of the detectors to obtain a long-term (weekly or monthly) average of the number concentration of ambient acidic particles may be expected to produce a manageable number of samples for a modestly equipped laboratory such as ours.

SUMMARY AND CONCLUSIONS

Iron nanofilm detectors are suitable for measuring the ambient concentration of acidic particles, except in extremely hot and humid conditions. During each of our sampling sessions, we exposed calibration samples that had previously generated acid reaction sites to filtered ambient air, with little apparent effect. The reaction sites, once formed, appeared stable. It would be of interest, however, to examine rates of reaction of acidic particles with the iron nanofilm in the presence of high concentrations of ambient gases, particularly ozone.

The number concentrations of ambient acidic particles were measured for the first time. The average concentrations ranged from approximately 100 to 1800 particles/cm^3 over our sampling periods.

The UDM system we used in these field tests required collection of an integrated sample over 1 to 2 weeks, providing an averaged particle concentration measurement. Our SMPS results showed that the airborne concentrations varied substantially with time. The high variability associated with the calculated mean particle concentrations made comparisons with the integrated sampling systems relatively qualitative. The total number concentrations of ultrafine particles measured on the iron nanofilm detectors exhibited the same trend as, but were somewhat lower than, the numbers measured with the SMPS system, indicating that the detector-AFM system underestimated the particle number concentration.

The fraction of ultrafine particles that were acidic varied from approximately 10% to 88% over the different seasons and sites. Size-segregated particle samples analyzed by ion chromatography showed that most of the H^+ occurred in the size fraction with diameters between 280 and 530 nm, but the relative acidity was greater for particles less than 88 nm in diameter. The number of acidic ultrafine particles did not correlate with the H^+ content of the size fraction for these sampling sessions.

The ability to monitor ultrafine acidic particles provided by these detectors enlarges the array of air quality variables that can be measured. This may help to resolve some of the outstanding questions related to causal relations between demonstrated health effects of ambient particles and PM components.

ACKNOWLEDGMENTS

The authors thank Dr Judy Xiong, who built the system, for producing highly controlled monodisperse H_2SO_4 particles; Jonghun Jung for assistance in measuring the deposition efficiency in the UDMs; and Gordon Cook, who prepared many of the final graphics. Ms Toni Moore and Ms Francine Lupino assisted with preparation of the report. This work is part of Center Programs supported by grants from the EPA (827351) and the National Institute of Environmental Health Sciences (ES00260).

REFERENCES

Amdur MO, Chen LC. 1989. Furnace-generated acid aerosols: Speciation and pulmonary effects. Environ Health Perspect 79:147–150.

Appel BR. 1993. Atmospheric sample analysis and sampling artifacts. In: Aerosol Measurement: Principles, Techniques, and Applications (Willeke K, Baron PA, eds). Van Nostrand Reinhold, New York NY.

Bates DV, Sizto R. 1987. Air pollution and hospital admissions in southern Ontario: The acid summer haze effect. Environ Res 43:317–331.

Brauer M, Koutrakis P, Keeler GJ, Spengler JD. 1991. Indoor and outdoor concentrations of inorganic acidic aerosols and gases. J Air Waste Manage Assoc 41:171–181.

Brauer MA, Koutrakis P, Wolfson MJ, Spengler JD. 1989. Evaluation of the gas collection of an annular denuder system under stimulated atmospheric conditions. Atmos Environ 23:1981–1986.

Cadle SH, Countess RJ, Kelly NA. 1982. Nitric acid and ammonia in urban and rural locations. Atmos Environ 16:2501–2506.

Chen LC, Wu CY, Qu QS, Schlesinger RB. 1995. Number concentration and mass concentration as determinants of

biological response to inhaled irritant particles. Inhalation Toxicol 7:577–588.

Cheng YS. 1995. Denuder systems and diffusion batteries. In: Air Sampling Instruments for Evaluation of Atmospheric Contaminants, 8th edition (Cohen BS, Hering SV, eds). American Conference of Governmental Industrial Hygienists, Cincinnati OH.

Cohen BS, Li W, Xiong JQ, Lippmann M. 2000. Detecting H^+ in ultrafine ambient aerosol using iron nano-film detectors and scanning probe microscopy. Appl Occup Environ Hyg 15:80–89.

Dockery DW, Cunningham J, Damokosh AI, Neas LM, Spengler JD, Koutrakis P, Ware JH, Raizenne M, Speizer FE. 1996. Health effects of acid aerosols on North American children: Respiratory symptoms. Environ Health Perspect 104:500–505.

Dockery DW, Damokosh AI, Neas LM, Raizenne M, Spengler JD, Koutrakis P, Ware JH, Speizer FE. 1993. Health effects of acid aerosols on North American children: Respiratory symptoms and illness (abstract). Am Rev Respir Dis 147:A633.

Dockery DW, Speizer FE, Stram DO, Ware JH, Spengler JD, Ferris BG Jr. 1989. Effects of inhalable particles on respiratory health of children. Am Rev Respir Dis 139:587–594.

Driscoll KE. 1994. Macrophage inflammatory proteins: Biology and role in pulmonary inflammation. Exp Lung Res 20:473–490.

Environmental Protection Agency (US). 1996. Air Quality Criteria for Particulate Matter, Volume 1. EPA/600/P-95/001aF. National Service Center for Environmental Publications, Cincinnati OH.

Hattis D, Abdollahzadeh S, Franklin CA. 1990. Strategies for testing the "irritation-signaling" model for chronic lung effects of fine acid particles. J Air Waste Manage Assoc 40:322–330.

Hattis D, Wasson JM, Page GS, Stern B, Franklin CA. 1987. Acid particles and the tracheobronchial region of the respiratory system: An "irritation-signaling" model for possible health effects. J Air Pollut Control Assoc 37:1060–1066.

Haward CN, McClenny WA, Hoell JM, Williams JA, Williams BS. 1982. Ambient ammonia measurement in coastal southeastern Virginia. Atmos Environ 16:2497–2500.

Hinds WC. 1982. Aerosol Technology: Properties, Behavior, and Measurement of Airborne Particles. John Wiley & Sons, New York NY.

Hinds WC. 1999. Aerosol Technology: Properties, Behavior, and Measurement of Airborne Particles, 2nd edition. John Wiley & Sons, New York NY.

Huang P-F, Turpin B. 1996. Reduction of sampling and analytical errors for electron microscopic analysis of atmospheric aerosols. Atmos Environ 30:4137–4148.

John W. 1993. The characteristics of environmental and laboratory-generated aerosols. In: Aerosol Measurement: Principles, Techniques, and Applications (Willeke K, Baron PA, eds). Van Nostrand Reinhold, New York NY.

Kamens R, Lee CT, Wiener R, Leith D. 1991. A study to characterize indoor particles in three non-smoking homes. Atmos Environ 25:939–948.

Koenig JQ, Covert DS, Pierson WE. 1989. Effects of inhalation of acidic compounds on pulmonary function in allergic adolescent subjects. Environ Health Perspect 79:173–178.

Koenig JQ, Pierson WE, Horike M. 1983. The effects of inhaled sulfuric acid on pulmonary function in adolescent asthmatics. Am Rev Respir Dis 128:221–225.

Koutrakis P, Wolfson JM, Spengler JD. 1988. An improved method for measuring aerosol acidity: Results from nine-month study in St Louis, Missouri and Kingston, Tennessee. Atmos Environ 22:157–162.

Leikauf GD, Spektor DM, Albert RE, Lippmann M. 1984. Dose-dependent effects of submicrometer sulfuric acid aerosol on particle clearance from ciliated human lung airways. Am Ind Hyg Assoc J 45:285–292.

Lippmann M. 1989. Background on health effects of acid aerosols. Environ Health Perspect 79:3–6.

Lippmann M, Ito K. 1995. Separating the effects of temperature and season on daily mortality from those of air pollution in London: 1965–1972. Inhalation Toxicol 7:85–97.

Lippmann M, Ito K, Nádas A, Burnett RT. 2000. Association of Particulate Matter Components with Daily Mortality and Morbidity in Urban Populations. Research Report 95. Health Effects Institute, Cambridge MA.

Lippmann M, Thurston GD. 1996. Sulfate concentrations as an indicator of ambient particulate matter air pollution for health risk evaluations. J Expos Anal Environ Epidemiol 6:123–146.

Liu BYH, Whitby KT, Yu HHS. 1967. Electrostatic aerosol sampler for light and electron microscopy. Rev Sci Instrum 38:100–102.

Marple VA, Rubow KL, Behm SM. 1991. A Microorifice Uniform Deposit Impactor (MOUDI): Description, calibration, and use. Aerosol Sci Technol 14:434–446.

National Research Council (US). 1977. Airborne Particles. National Academy Press, Washington DC.

Oberdörster G, Ferin J, Gelein R, Soderholm SC, Finkelstein J. 1992. Role of the alveolar macrophage in lung injury: Studies with ultrafine particles. Environ Health Perspect 97:193–199.

Oberdörster G, Finkelstein JN, Johnson C, Gelein R, Cox C, Baggs R, Elder ACP. 2000. Acute Pulmonary Effects of Ultrafine Particles in Rats and Mice. Research Report 96. Health Effects Institute, Cambridge MA.

Oberdörster G, Gelein RM, Ferin J, Weiss B. 1995a. Association of particulate air pollution and acute mortality: Involvement of ultrafine particles? Inhalation Toxicol 7:111–124.

Oberdörster G, Seaton AW, MacNee K, Donaldson D, Godden D. 1995b. Particulate air pollution and acute health effects. Lancet 345:176–178.

Ostro BD, Lipsett MJ, Wiener MB, Selner JC. 1991. Asthmatic responses to airborne acid aerosols. Am J Public Health 81:694–702.

Owen MK, Ensor DS, Hovis LS, Tucker WG, Sparks LE. 1990. Particle size distributions for an office aerosol. Aerosol Sci Technol 13:486–492.

Owen MK, Ensor DS, Sparks LE. 1992. Airborne particle sizes and sources found in indoor air. Atmos Environ 26A:2149–2162.

Ozkaynak H, Thurston GD. 1987. Associations between 1980 US mortality rates and alternative measures of airborne particle concentration. Risk Anal 7:449–461.

Pasternack BS, Harley NH. 1971. Detection limits for radionuclides in the analysis of multi-component gamma ray spectrometer data. Nuclear Instrum Methods 91:533.

Penttinen P, Timonen KL, Tiittanen P, Mirme A, Ruuskanen J, Pekkanen J. 2001. Number concentration and size of particles in urban air: Effects on spirometric lung function in adult asthmatic subjects. Environ Health Perspect 109:319–323.

Peters A, Dockery DW, Heinrich J, Wichmann HE. 1997a. Medication use modifies the health effects of particulate sulfate air pollution in children with asthma. Environ Health Perspect 105:430–435.

Peters A, Wichmann H-E, Tuch T, Heinrich J, Heyder J. 1997b. Respiratory effects are associated with the number of ultrafine particles. Am J Respir Crit Care Med 155:1376–1383.

Possanzini M, Febo A, Liberti A. 1983. New design of a high-performance denuder for the sampling of atmospheric pollutants. Atmos Environ 17:2605–2610.

Raizenne M, Neas LM, Damokosh AI, Dockery DW, Spengler JD, Koutrakis P, Ware JH, Speizer FE. 1996. Health effects of acid aerosols on North American children: Pulmonary function. Environ Health Perspect 104:506–514.

Samet JM, Dominici F, Zeger SL, Schwartz J, Dockery DW. 2000a. The National Morbidity, Mortality, and Air Pollution Study, Part I: Methods and Methodologic Issues. Research Report 94. Health Effects Institute, Cambridge MA.

Samet JM, Zeger SL, Dominici F, Curriero F, Coursac I, Dockery DW, Schwartz J, Zanobetti A. 2000b. The National Morbidity, Mortality, and Air Pollution Study, Part II: Morbidity and Mortality from Air Pollution in the United States. Research Report 94. Health Effects Institute, Cambridge MA.

Seaton A, MacNee W, Donaldson K, Godden D. 1995. Particulate air pollution and acute health effects. Lancet 345:176–178.

Shaw RW, Stevens RK, Bowermaster J, Tesch JW, Tew E. 1982. Measurements of atmospheric nitrate and nitric acid: The denuder difference experiment. Atmos Environ 16:845–853.

Spektor DM, Yen BM, Lippmann M. 1989. Effect of concentration on cumulative exposure of inhaled sulfuric acid on tracheobronchial particle clearance in healthy humans. Environ Health Perspect 79:167–172.

Spengler JD, Brauer M, Koutrakis P. 1990. Acid air and health. Environ Sci Technol 24:946–956.

Thurston GD, Ito K, Hayes CG, Bates DV, Lippmann M. 1994. Respiratory hospital admissions and summertime haze air pollution in Toronto, Ontario: Consideration of the role of acid aerosols. Environ Res 65:271–290.

Utell MJ, Morrow PE, Speers DM, Darling J, Hyde RW. 1983. Airway responses to sulfate and sulfuric acid aerosols in

asthmatics: An exposure-response relationship. Am Rev Respir Dis 128:444–450.

Whitby KT, Husar RB, Liu BYH. 1972. The aerosol size distribution of Los Angeles smog. J Colloid Interface Sci 39:177–204.

Wichmann H-E, Peters A. 2000. Epidemiological evidence of the effects of ultrafine particle exposure. Phil Trans R Soc Lond Ser A 358:2751–2769.

Wichmann H-E, Spix C, Tuch T, Wölke G, Peters A, Heinrich J, Kreyling WG, Heyder J. 2000. Daily Mortality and Fine and Ultrafine Particles in Erfurt, Germany, Part 1: Role of Particle Number and Particle Mass. Research Report 98. Health Effects Institute, Cambridge MA.

Xiong JQ, Zhong M, Fang CP, Chen LC, Lippmann M. 1998. Influence of organic films on the hygroscopicity of ultrafine sulfuric acid aerosol. Environ Sci Technol 32:3536–3541.

ABOUT THE AUTHORS

Beverly S Cohen is a professor of environmental medicine at NYU School of Medicine. She serves as director of the NYU School of Medicine National Institute of Environmental Health Sciences Center's Shared Resource in Inhalation and Exposure Assessment and of the Exposure, Dosimetry, and Modelling Research Core of the EPA PM_{10} Center. Cohen received her PhD in Environmental Health Sciences from NYU in 1979, her MS in Radiological Physics from Cornell University Graduate School of Medical Sciences in 1961, and her BS in Physics from Bryn Mawr College in 1953. Her research interests include measurement of personal exposures to airborne toxicants, dosimetry of inhaled pollutant gases and aerosols, airborne radioactivity, and development of biomarkers for assessment of personal exposure.

Maire Heikkinen received her PhD in Environmental Health Sciences at NYU's Institute of Environmental Medicine in 1997. Her interests are in measurement of ultrafine and nanometer aerosols and development of instrumentation for collection and analysis of acidic, radioactive, and biological particles. She is currently a research assistant professor of environmental medicine.

Yair Hazi received his PhD in Environmental Health Sciences at NYU's Institute of Environmental Medicine in 2001. He is currently a postdoctoral research scientist in the Division of Environmental Health Sciences at Columbia University. His research interests include documentation of human exposure to airborne contaminants.

Hai Guo is currently a research fellow at the Hong Kong Polytechnical University Research Center for Urban Environment. He earned his PhD in Environmental Science at Murdoch University, Perth, Australia in 1999 and then was a postdoctoral fellow at NYU. He holds an MS in Chemistry from Wuhan University in China. His research interest is in airborne toxicants.

Morton Lippmann is professor of environmental medicine at NYU School of Medicine. He is also director of the Human Exposure and Health Effects Research Program of the Department of Environmental Medicine and the Particulate Matter Health Effects Research Center at NYU and is supported by grant R827351 from the EPA. He received a BchE from the Cooper Union in 1954, an SM in Industrial Hygiene from Harvard University in 1955, and a PhD in Environmental Health Sciences from NYU in 1967. His research interests focus on exposure assessment and the health effects of airborne toxicants.

ABBREVIATIONS AND OTHER TERMS

AFM	atomic force microscopy
CNC	condensation nuclei counter
EAS	electrostatic aerosol sampler
E_f	particle collection efficiency
EPA	Environmental Protection Agency (US)
H^+	hydrogen ion
H_2SO_4	sulfuric acid
HNO_3	nitric acid
MOI	microorifice impactor
NaCl	sodium chloride
NH_3	ammonia
NH_4^+	ammonium
NIEM	Nelson Institute of Environmental Medicine
NYC	New York City
NYU	New York University
P	penetration efficiency
PM	particulate matter
PM_{10}	PM 10 µm or less in aerodynamic diameter
$PM_{2.5}$	PM 2.5 µm or less in aerodynamic diameter
PSL	polystyrene latex
Q	flow rate

r^2	coefficient of determination for bivariate analysis
RFA	Request for Applications
RH	relative humidity
SMPS	scanning mobility particle sizer
SO_2	sulfur dioxide
SO_4^{2-}	sulfate
UDM	ultrafine diffusion monitor

CRITIQUE
Health Review Committee

INTRODUCTION

Over the last several decades, evidence has accumulated suggesting that exposure to airborne particulate matter (PM*), which includes particles from different sources and of varying size and composition, may affect the human cardiovascular and respiratory systems. Because of concerns about health effects, the US Environmental Protection Agency (EPA) regulates the ambient levels of PM through the National Ambient Air Quality Standards, which were revised in 1997 (EPA 1997) and are currently being reevaluated. Ambient particles tend to fall in a trimodal size distribution by aerodynamic diameter: coarse particles (greater than 1000 nm), fine particles (100 to 1000 nm), and ultrafine particles (less than 100 nm). Although ultrafine particles constitute a small percentage of the total PM mass in the size regulated by the EPA (PM less than 2.5 μm in aerodynamic diameter), they are present in high number concentrations.

In order to understand the health effects of PM components and thus to inform decisions on ambient PM standards and pollution control strategies, considerable research has been conducted. Some components that have been studied are transition metals (known to be involved in oxidation-reduction reactions), ultrafine particles (more likely than larger particles to deposit in the lung, escape phagocytosis, and translocate to lung tissues and other organs), and acidic particles (may affect lung function and increase respiratory symptoms in asthmatic persons). Research has been limited, however, by the lack of instruments that can measure the levels of specific PM components. To address this need, a number of new particulate samplers that measure different combinations of particle components, or particles of different sizes, have been developed in the past several years. Evaluation of new PM samplers is complex and costly and is hampered by the lack of reference instruments that could be used to determine their accuracy directly. Comparison studies can be used to evaluate the extent of agreement between different types of monitors and the reliability of the measurements (EPA 1997).

In 1998, HEI issued RFA 98-1, "Characterization of Exposure to and Health Effects of Particulate Matter," seeking studies to improve characterization of personal exposure to PM and to evaluate biological mechanisms of effects of PM exposure and attributes of particles that may cause toxicity. In response to this RFA, Dr Beverly Cohen and colleagues at New York University Medical Center proposed to test a new iron-coated nanofilm for collecting and measuring ambient concentrations of acidic ultrafine PM, both outdoors and indoors. Preliminary data presented in the application indicated that laboratory-generated acidic particles reacted with the iron on the nanofilm surface producing distinct ringed reaction sites that could be visualized and counted using atomic force microscopy (AFM) (Cohen et al 2000). For collecting the airborne particles, the investigators planned to place the iron nanofilms in two samplers that differed in their size selectivity and operating parameters. Because no method was currently available for comparison in measuring acidic ultrafine particles, Dr Cohen proposed to compare the measurements made with the iron nanofilm detector system to the strong acidity content of particles of similar size collected on filters used with the microorifice impactor (MOI), a common PM sampler that separates and collects PM of different sizes. The HEI Research Committee recommended funding this proposal because they thought it would be useful to obtain information on the level of acidic ultrafine particles in the environment.† This Critique is intended to aid HEI sponsors and the public by highlighting the strengths of the study, pointing out alternative interpretations, and placing the research into scientific perspective.

SCIENTIFIC BACKGROUND

HEALTH EFFECTS OF ULTRAFINE PM

Ultrafine particles are generally present in the ambient air in two modes. The nucleation mode (PM < 50 nm) comprises mostly volatile organic material and sulfate. The accumulation mode (PM 50 to 300 nm), which extends into the fine fraction, contains agglomerated material such as elemental and organic carbon, nitrate, sulfate, and various metallic ashes.

(Although the definition of ultrafine particles usually refers to particles less than 100 nm, in this report the

* A list of abbreviations and other terms appears at the end of the Investigators' Report.

This document has not been reviewed by public or private party institutions, including those that support the Health Effects Institute; therefore, it may not reflect the views of these parties, and no endorsements by them should be inferred.

† Dr Cohen's 2-year study, "Assessment of H^+ and Ultrafine Particles in Indoor and Outdoor Air," began in October 1998. Total expenditures were $367,000. The draft Investigators' Report from Cohen and colleagues was received for review in January 2002. A revised report, received in April 2003, was accepted for publication in June 2003. During the review process, the HEI Health Review Committee and the investigators had the opportunity to exchange comments and to clarify issues in both the Investigators' Report and in the Review Committee's Critique.

authors used it in some cases to include particles up to 300 nm in diameter.) Particles from mobile sources are generally present in the form of fine and ultrafine PM.

At the time the study was funded in 1998, little information had been published on the effects of inhaling ambient ultrafine particles. Scientists had proposed, however, that ultrafine particles could be responsible for some of the adverse effects observed in epidemiologic studies (Seaton et al 1995; Donaldson et al 1998; Mauderly et al 1998). Seaton and colleagues (1995) hypothesized that greater retention of inhaled ultrafine particles, relative to larger particles, leads to inflammation and exacerbation of existing pulmonary and cardiovascular diseases. Experimental studies using resuspended particles provided some evidence that at the same mass concentration as fine particles, ultrafine particles caused greater lung inflammation (Ferin et al 1992). This finding was attributed to the larger surface area of ultrafine particles (Oberdörster et al 1992). Donaldson and coworkers (1998) subsequently showed that instilled ultrafine particles of different compositions had different potencies in causing inflammation and oxidative stress. Studies modeling particle deposition have indicated that ultrafine particles are more likely to be deposited in the lower respiratory tract. At the same time, they are less likely to be phagocytized by alveolar macrophages and cleared by mucociliary action than larger particles. Thus ultrafine particles have more potential to migrate to lung tissues and other organs (Kreyling and Scheuch 2000).

HEALTH EFFECTS OF ACIDIC PM

By 1998, when this study was funded, many epidemiologic and experimental studies had already been published on the effects of coarse and fine acidic particles (see reviews by Amdur 1996; Speizer 1999; Schlesinger and Cassee 2003). Only a few studies, however, had evaluated the effects of ultrafine acidic particles. Experiments with high concentrations of fine sulfuric acid particles showed an increase in airway hyperresponsiveness of asthmatic human subjects in some studies and consistently in studies of rabbits (Schlesinger and Cassee 2003). No effects were observed in healthy human subjects. Studies in a variety of species found that exposure to fine sulfuric acid particles decreased or increased mucociliary clearance, depending on the dose and the airway region examined (Amdur 1989). In studies of guinea pigs, sulfuric acid–coated ultrafine particles (zinc oxide) caused changes in epithelial cell permeability, pulmonary edema, and a decrease in the lungís capacity for diffusing carbon monoxide (a measure of impairment of blood oxygenation) at concentrations lower than those of pure sulfuric acid aerosol that elicited these effects (Amdur and Chen 1989).

Time-series epidemiologic studies showed a consistent association between summertime ambient acidity and hospital admissions for asthma and other respiratory diseases (Speizer 1999). Studies on the association between acidity and changes in lung function in children yielded some positive and some negative results (Speizer 1999). These studies, however, measured acidity in coarse and fine particles only.

FORMATION OF ACIDIC PM

Particulate matter consists of primary particles generated directly from sources and secondary particles (such as sulfate and nitrate) formed by reactions that occur in the atmosphere. Sulfuric acid and nitric acid, for example, are produced by gas-to-particle conversion of sulfur dioxide and nitrogen dioxide, respectively, in the presence of hydroxyl radicals. Once formed, these liquid particles either condense on preexisting particles or combine with each other to form new particles. They generally exist in the ultrafine particle fraction when first formed and ultimately in the fine or coarse fraction (Schlesinger and Cassee 2003). When sulfuric acid production is high and the existing PM concentration is low, a large number of new nuclei mode sulfate particles can be formed, contributing significantly to the total number concentration (NARSTO 2003). If ammonia is present, it can react with, and neutralize, the acidic aerosols.

MEASURING PARTICLE CHARACTERISTICS

Instruments measuring PM generally have two components: one collects particles within a certain size range, and the other analyzes the selected particles. All PM samplers are equipped with a pump drawing air through an inlet that defines the upper size of the particles that are collected. Different instruments use different methods for collecting and classifying the particles, exploiting a variety of particle features such as weight, shape, density, and refractive index. For example, impactors, cyclones, and aerodynamic particle sizers classify particles according to aerodynamic diameter, which depends on their density, shape and size; mobility analyzers segregate and classify particles according to their electrical mobility, which depends on their shape and size; and diffusion monitors separate particles by their diffusion coefficient, which depends on their size only (NARSTO 2003). Coarse particles and, to a lesser extent, fine particles can be separated aerodynamically; smaller particles can be separated by diffusion deposition.

There are two general approaches to analyzing PM. One approach is to analyze PM collected on a substrate over a certain period of time (integrated measure). This analysis is limited in terms of time resolution, and its results may be biased by sampling artifacts, such as losses or gains of semivolatile components; however, it offers the advantage of collecting sufficient material for analysis of components present in small amounts. The other approach is to analyze PM in situ, yielding continuous, real-time measurements of some its components.

Several research groups have reviewed the instruments available for particle measurements (Burtscher 2001; Schwela et al 2002; NARSTO 2003). The following sections describe only the instruments used in the Cohen study to collect and analyze particles and to measure their number.

For integrated analysis of size-segregated particle composition, the MOI is routinely used. This instrument consists of a size-specific inlet and a number of impactor plates in series, each with different and progressively smaller cutoff diameters, which collect smaller and smaller particles. Mobility analyzers and diffusion monitors, such as the electrical aerosol sampler (EAS) and the ultrafine diffusion monitor (UDM) used in the Cohen study, also can be utilized to collect particles on a substrate for chemical analysis. The EAS precipitates particles ranging in size from approximately 3 to 700 nm by charging them. The UDM relies on the diffusive properties (due to Brownian motion) of ultrafine particles, whereby the particles adhere when they hit a surface (Knuston 1999). Collected particles can be weighed and chemically analyzed for a variety of characteristics or components (such as acidity, ionic species, organic compounds, and metals). To determine particle acidity, filter samples are analyzed by extraction followed by a pH measurement. Often relatively long sample periods are required to obtain sufficient material for reliable analysis (Schwela et al 2002).Total number concentration is generally measured continuously by condensation nuclei counters (CNCs) or condensation particle counters. Because ultrafine particles heavily influence the total particle number concentration, these instruments have been specifically designed to detect such particles by growing them into large droplets in an atmosphere saturated with *n*-butanol. The droplets are detected by a laser light source that can count particles down to 3 nm in diameter (Schwela et al 2002). The two counters work on the same general principle, but differ slightly in their design and operating characteristics. These instruments are very versatile and can provide number-weighted size distribution data when used in combination with particle sizers before they undergo condensation. A scanning mobility particle sizer (SMPS), an instrument consisting of both a differential mobility analyzer, which separates particles by size by sequentially increasing the electric field, and a CNC, was used by Cohen and colleagues for comparison measurements of total particle number.

TECHNICAL EVALUATION

STUDY DESIGN AND OBJECTIVES

Cohen and colleagues hypothesized that because small particles are more likely than larger particles to deposit in the lower respiratory tract, and particle acidity is known to damage lung tissues, acidic ultrafine particles may be especially toxic. However, none of the existing sampling methods could provide a direct measure of these particles. This 2-year study aimed at evaluating an iron nanofilm detector system for measuring the number concentration of acidic ultrafine particles in ambient air. The iron nanofilm had been previously tested under laboratory conditions using laboratory-generated acidic particles (Cohen et al 2000) and showed promise for its application to field sampling.

The authors tested the performance of the iron nanofilms under a variety of storage conditions and deployed them in two samplers, the MOI-EAS system and the UDM, to obtain time-integrated measurements of acidic ultrafine particles and total ultrafine particles in outdoor and indoor locations. In most of the field monitoring sessions, two commercially available instruments that measure particle number concentrations, the SMPS and the CNC, were also deployed for purposes of comparison and quality control. Specifically, the study set out to address the following main objectives:

1. Determine the stability of the iron nanofilm at high temperature and humidity over time.
2. Measure and compare the number concentrations of acidic particles and total ultrafine particles determined using the iron nanofilms deployed in the MOI-EAS and the UDM, at rural and urban outdoor sites during different seasons and in indoor microenvironments.
3. Compare the number of acidic ultrafine particles measured using the iron nanofilms in the MOI-EAS with the acid content of particles of comparable size collected on MOI filters.
4. Compare the total ultrafine particle concentrations (of acidic and nonacidic particles) determined using the iron nanofilms in the MOI-EAS and the UDM with those determined using the SMPS.

METHODS

Visualization of Particles on Iron Nanofilms

The iron nanofilm, a thin iron-coated silicon chip (5 mm × 5 mm × 0.6 mm) was used as the collection substrate. The investigators assumed that, upon impaction, each acid particle would react with the iron creating an elevated site, or bump, on the film surface. They visualized the reaction sites using an atomic force microscope equipped with a nanometer-size vibrating tip that maps the surface topography of the film without making contact. AFM produces a colored scan of the surface on which light spots represent the elevated sites resulting from the reaction of acidic particles with iron. As shown in this report and in previous work (Cohen et al 2000), laboratory-generated acidic particles generally formed reaction sites surrounded by a ring, or halo. Therefore, elevated sites with rings on iron nanofilm detectors exposed to ambient aerosol were assumed to reflect acidic particles. Sites without rings were assumed to represent nonacidic particles that had deposited on the nanofilm. For the purpose of determining the stability of the reaction sites, the diameter of the central (highest) peak was calculated. Particles with diameters less than 30 to 35 nm yielded sites that were not detectable with the protocol used for these AFM scans.

Evaluation of Iron Nanofilm Performance

The following aerosols of different sizes were generated for calibration purposes, for determination of deposition efficiency, or for quality control procedures: sulfuric acid particles (35, 64, and 141 nm in diameter), polystyrene latex microspheres (50, 88, 126, and 198 nm in diameter), sodium chloride particles (75 and 150 nm), and fluorescein particles (50 and 100 nm).

Iron nanofilm performance was tested using both unexposed (blank) nanofilms and nanofilms previously exposed to standard sulfuric acid particles of different diameters. The EAS was used to precipitate particles onto the nanofilms. The stability of the nanofilm surface and of the reaction sites during storage was tested as a function of time (up to 18 months) under nitrogen at room temperature and as a function of temperature at high humidity (88% relative humidity at 39°C or 92% relative humidity at 22°C) for 3 months. The effects of weather conditions and gaseous pollutants were evaluated by placing sealed aluminum canisters containing blank nanofilms and previously exposed nanofilms in the field for 1 week. The canisters had a membrane filter at the inlet and were connected to a pump drawing ambient air.

Field Monitoring Samplers

For ambient air sampling, the iron nanofilms were deployed in two different sampling systems, the MOI-EAS and the UDM, and the SMPS and CNC were used to obtain comparison measurements (see Critique Table 1).

MOI-EAS This system consisted of the combination of an eight-stage MOI and an EAS, which housed the iron nanofilms. Two annular denuders to remove ammonia, nitrate, and sulfur oxide were placed before the MOI. The purpose of the MOI was to select the size of particles entering the EAS. For this study the last (eighth) stage of the MOI was removed, and the flow after the seventh stage (with a cut size of 88 nm) was split, with one part directed to the EAS for collection of particles on pairs of iron nanofilms and the other part directed to a polycarbonate filter for subsequent analysis of particle acidity. The average particle-deposition efficiency on the filter after the last stage of the MOI was 76% (determined using sodium chloride particles of different sizes). The average deposition efficiency of the EAS, as determined using polystyrene latex microspheres, was 66% (owing to the fact that not all particles acquire an electric charge and are deposited on the nanofilm). For all outdoor sampling sessions, the investigators analyzed the particles collected at each MOI stage for hydrogen, sulfate, and ammonium ions (which required extraction in aqueous

Critique Table 1. Characteristics of the Particle Samplers Used in the Study

Sampler	Particle Size Range (nm)	Flow Rate[a] (L/min)	Deposition Efficiency (%)
MOI-EAS/ nanofilm	40–100	15	77 (MOI filter) 66 (EAS)
UDM/ nanofilm	40–300 estimated (no size-selective inlet)	0.01 0.2	$7.1–7.5 \times 10^{-7}$ 7.7×10^{-8}
SMPS	35–100 (for comparison with MOI-EAS) 40–300 (for comparison with UDM)	1	89–97
CNC	7–1000 (no size-selective inlet)	0.3	90[b]

[a] In the Investigators' Report the UDM flow rates are presented as 10 cm^3/min and 200 cm^3/min.

[b] Efficiency with which particles penetrate the inlet tube.

solution followed by ion chromatography) to provide a size distribution of these components.

UDM The UDM draws air at a low flow rate through a narrow space between two parallel plates. Through Brownian motion (diffusion) the particles hit the plates' walls and deposit on pairs of iron nanofilm detectors placed at three locations along their length. The deposition efficiency depends on the distance from the inlet and the flow rate. Two flow rates were used in the field tests, 10 cm^3/min and 200 cm^3/min. Because of low particle deposition downstream, only the two detectors closest to the air flow intake were used for particle counts. The average deposition efficiency, determined experimentally with fluorescein particles using aluminized Mylar as a collection substrate, was 7.1 to 7.5 $\times 10^{-7}$% at 10 cm^3/min and 7.7 $\times 10^{-8}$% at 200 cm^3/min.

SMPS During all sampling sessions, the SMPS was deployed to provide size-classified particle counts for comparison with the total ultrafine particle counts determined with the MOI-EAS and UDM. In comparisons with the MOI-EAS data, the SMPS measurements were averaged for particles between 35 and 100 nm in size; in comparisons with the UDM data, they were averaged for particles between 40 and 300 nm in size. The SMPS results were corrected for estimated losses of about 10% through the sampling line (approximately 9 m in length).

CNC Total particle counts were provided by the CNC for some of the sampling sessions. This instrument was used to obtain additional measures for quality control, in particular, to compare with the SMPS determinations. It had an upper size cutoff of approximately 1 μm (B Cohen, personal communication).

Field Monitoring Sessions

Field sampling sessions were conducted during each of the four seasons in a rural area (Tuxedo NY) between July 1999 and May 2000 and during the winter of 2000 in an urban area (New York City). For these tests the MOI-EAS and the UDM were collocated. The MOI-EAS sampled continuously for two consecutive 1-week periods (yielding two measures for each season). In the rural area, the UDM sampled for two consecutive 1-week periods in the summer, for a 1-week and a 2-week period in the fall and winter, and for one 2-week period in the spring. Moreover, in the winter and spring sessions, two UDMs were used, one operating at the same flow rate as the previous sessions (10 cm^3/min) and the other operating at a higher flow rate (200 cm^3/min). In New York City, the UDM sampled for two consecutive 1-week periods. As in the winter sampling in Tuxedo, two UDMs operating at different flow rates were used. The SMPS and the CNC were run in parallel to the MOI-EAS and the UDM for the same sampling periods. The samplers were housed in either a stainless steel unit or a shed.

The UDM was deployed also in two indoor environments: the cafeteria at the Nelson Institute of Environmental Medicine (NIEM) in Tuxedo and a residence in Newburgh. A second UDM measured outdoor levels at both sites. The SMPS and the CNC were used for the NIEM cafeteria sampling. The SMPS sampled alternatively indoor and outdoor air, while the CNC sampled only indoor air.

During the sampling sessions, blank nanofilms and nanofilms preexposed to acidic particles were deployed in canisters that sampled ambient air filtered through a membrane inlet. This process allowed determination of the effects of exposure to ambient gases on the nanofilm surface and the reaction sites.

Data Analysis

Acidic particles and total particles were counted on the nanofilm areas scanned by AFM, which corresponded to 6.4×10^{-3}% (four areas in each of the four quadrants) or 1.6×10^{-3}% (two areas in each of two quadrants) of the total available surface. Particle number concentration was calculated from the counts on the scanned areas, taking into account the total surface of the nanofilm, the particle collection efficiency, the volume of air sampled, and other parameters specific to the sampler. For the MOI-EAS calculations, only the collection efficiency in the EAS was used; losses in the MOI were not accounted for. The data presented represent the average of determinations made on pairs of detectors.

RESULTS

Iron Nanofilm Performance

Storage of the iron nanofilms under nitrogen for up to 18 months did not significantly alter the surface of either blank detectors or detectors preexposed to acidic particles. The storage may have caused a small increase in the diameter of the central peak of some reaction sites for the 64-nm standard sulfuric acidic particles (based on monthly analysis of a small number of sites).

Storage for 3 months at high humidity (88% relative humidity) and high temperature (39°C) caused corrosion and increased roughness of the nanofilm surface and enlargement of the sites on nanofilms with a high density of acidic particles. Storage at a similar high humidity (92%)

and lower temperature (22°C) did not affect the surface of the film, but caused some enlargement of the reaction sites.

Blank nanofilms placed in the filtered air canisters and exposed only to ambient gases during the field sampling sessions did not display any surface changes. Nanofilms preexposed to laboratory-generated sulfuric acid particles showed enlargements of the spots at the end of one of the field sessions relative to the size measured immediately after the initial exposure. However, because AFM did not permit selection of the same areas that were previously scanned, all these temporal observations were made in different areas of the film.

Outdoor Measurements

MOI-EAS and UDM Results There was a large difference in the concentrations of acidic ultrafine particles measured by the MOI-EAS and those measured by the UDMs during the outdoor sampling sessions. Moreover, although the UDM performance varied with the sampling flow rate, there was no consistent trend wherein one instrument (MOI-EAS or UDM) or one UDM flow rate gave a higher or lower concentration of acidic ultrafine particles. The total numbers of particles determined with the two samplers also differed (Critique Table 2). The MOI-EAS values were consistently lower than the UDM values. The percentage of acidic ultrafine particles relative to total ultrafine particles was different for the two instruments. In the samples collected with the MOI-EAS in New York City, around 10% of the total particles were acidic; in the samples collected with the UDMs, 25% were acidic at the low flow rate and 3% at the high flow rate. At the rural Tuxedo site, between 19% and 88% of the total particles were acidic when determined with the MOI-EAS and between 0.2% and 25% when determined with the UDM. The highest proportion of acidic ultrafine particles in both locations was found in the fall and winter.

Comparison to Acidity and SMPS Measurements In the absence of an instrument that directly measures acidic ultrafine particles, the authors used the acidity (pH) of particles collected on the filter after the last stage of the MOI for comparison with the number of acidic ultrafine particles determined with the MOI-EAS. Samples from all of the monitoring sessions had similar levels of acidity, except for samples collected during the summer 2 session, when acidity was highest. In contrast, the number concentrations of acidic particles determined with the MOI-EAS showed more variability across the seasons. The summer 2 session, with the highest acidity, had a low number of

Critique Table 2. Total Number of Ultrafine Particles Determined with MOI-EAS, UDM, and the Reference SMPS

Sampling Sessions	MOI-EAS[a]	SMPS 35–100 nm[b]	UDM[c]	SMPS 40–300 nm[c]
Summer 1	621 ± 57	2400±1900	16,800 ± 9100	4313 ± 2306
Summer 2	603 ± 454	1900±1300	6400 ± 6100	2999 ± 1357
Fall 1	1072 ± 121	2500±1800	7400 ± 500	3296 ± 2246
Fall 2				
Fall 2+3	1070 ± 535	2600±1600	4800 ± 130	4043 ± 2357
Winter 1	1035 ± 60	3800±3400		
Winter 2	844 ± 233	4600±2700	3600 ± 2200[d]	6332 ± 3446
Winter 1+2			4800 ± 350	5917 ± 4451
Winter 3 (NYC)	1950 ± 560	9700±5500		
Winter 4 (NYC)	2763 ± 1412	11,200±6900		
Winter 3+4			7100 ± 70	11,405 ±7038
			22,000 ± 5600[d]	
Spring 1	516 ± 212	3700±2500		
Spring 2	605 ± 76	3800±3200		
Spring 1+2			7300 ± 4000	5137 ± 3285
			3900 ± 840[d]	

[a] Taken from Table 8 of the report.

[b] Taken from Figure 30 of the report.

[c] Taken from Table 10 of the report.

[d] UDM operating at the high flow rate.

acidic particles, and periods with very low acidity had the highest acidic particle counts.

The authors also compared the total number concentrations of particles determined by the MOI-EAS and the UDM with those obtained by the SMPS during the same sampling periods for the corresponding size ranges. In these comparisons all the MOI-EAS determinations were lower than those made with the SMPS, but some of the UDM results were in fairly good agreement with the SMPS determinations.

Indoor Measurements

Measurements taken inside the Newburgh residence with the UDM for an undefined period yielded number concentrations of acidic particles and total particles similar to those determined outdoors in Tuxedo. Indoors, acidic particles represented about 2% of the total particles. Measurements taken inside the NIEM cafeteria in Tuxedo yielded a similar concentration of total particles as in the Newburgh residence, but a 10-fold higher concentration of acidic particles. The concentration of acidic particles inside the cafeteria was 3-fold higher than the concentration outside.

Other Observations

Cohen and coworkers conducted additional studies to characterize the composition and size distribution of particles at the rural and urban sampling sites and to compare the performance of the CNC and SMPS, which were used to determine particle counts.

Analysis of MOI Filters Analysis of particles collected at each impactor stage of the MOI for hydrogen, sulfate, and ammonium ions showed that the highest levels of these components were in particles with an average (midpoint) diameter of 380 nm.

Number-Weighted Size Distribution of Airborne Particles The particle size distribution determined with the SMPS in Tuxedo was bimodal during the day, with both nuclei mode and accumulation mode particles, and unimodal at night, with accumulation mode particles. In New York City the distribution was essentially unimodal with nuclei mode particles throughout the whole sampling period. In Tuxedo, where monitoring was conducted during each of the four seasons, the particle number concentrations were higher in winter and spring than in summer and fall.

Comparison of SMPS and CNC Particle number concentration was determined for all sample sessions with both the SMPS and the CNC. The particle number concentrations were obtained by averaging the CNC recordings over a 1-hour period and the SMPS recordings over a 0.5-hour period. The agreement between the two instruments was relatively good at certain times of the day, but poor at other times. The SMPS yielded higher number concentrations than the CNC. The CNC values were not corrected for penetration losses, which were estimated to be around 10%. Though corrected CNC values would be higher, they would still be lower than the SMPS values.

DISCUSSION

The authors evaluated a novel iron nanofilm substrate for measuring acidic ultrafine particles. The rationale for the study was based on growing concern about the potential health effects of ultrafine particles and on the usefulness of distinguishing between acidic ultrafine and total ultrafine particles in epidemiologic studies. The study was carefully conducted and generally achieved the aims it set. The methods are well described and the results are clearly presented in numerous tables and figures.

The study evaluated the performance of iron-coated nanofilms in both laboratory and field conditions. For the field studies, the nanofilm was placed in the MOI-EAS and the UDM. The exposed nanofilms were examined by AFM, which produced a colored scan of the surface, on which light spots represented the elevated sites resulting from the reaction of particles with iron. With this method, particle size resolution depends on the scanning protocol and on the width and shape of the AFM scanning probe. In this study, particles smaller than 30 to 35 nm could not be identified. The authors believe that AFM also offers the potential to size particles by utilizing the information on height and width of the reaction sites. In order to make full use of the technology, however, more information is needed about how the actual size of the reaction sites relates to the original particle size and how the two dimensions provided by AFM vary with the size of acidic particles. When analyzing the iron nanofilms, Cohen and her colleagues assumed that acidic particles would form reaction sites with a ring and all other particles would form sites without a ring. They also assumed that the reaction was complete at the time of analysis and that the reaction sites remained stable once formed. However, the report does not provide sufficient data to verify these assumptions. Thus it is possible that certain particles were lost to analysis and some of the reaction sites were misclassified. Moreover, the size of the error introduced by the observer in counting the reac-

tion sites and how the count relates to particle type and size were not determined.

Laboratory experiments showed that the surfaces of both blank and preexposed nanofilms were generally stable for a storage period of 3 months, at average ambient temperature (22°C) and high humidity (92%), and were not affected substantially by exposure to particle-free ambient air. However, the surface appeared to deteriorate at high humidity when the storage temperature too was high (39°C). High humidity at both ambient temperature and high temperature at storage may have also caused enlargement of some reaction sites. The fact that the same areas of the detectors cannot be reexamined over time makes it difficult to evaluate temporal changes on the nanofilms.

The samplers chosen to house the iron nanofilms in the field studies differed in their collection methods and particle size selection. By charging the particles, the MOI-EAS had much greater deposition efficiency than the UDM, which relied on passive diffusion. Moreover, the MOI-EAS had a fairly sharp cutoff of 88 nm, while the UDM did not have a size-selective inlet. Coarse particles are present in very low number concentrations, however, and do not deposit by diffusion. Further, large particles on the nanofilm were not counted. Thus, the authors believe that, in practice, the particles counted on the nanofilm in the UDM were less than 300 nm in diameter and that the majority of those counted were actually smaller than 100 nm. This assumption is probably correct but was not proven experimentally.

The results of the monitoring studies showed limited agreement between the MOI-EAS and UDM samplers. There was no trend in the relation of acidic particle numbers measured by the two instruments. For the total particle number concentrations, however, the MOI-EAS consistently yielded lower values than those obtained with the UDMs at either flow rate. The poor agreement between the two types of samplers may be due, at least in part, to their different characteristics. While the UDM would be expected to yield higher numbers of particles because it lacks a size-selective inlet, its lower deposition efficiency may tend to bias the results downward. Moreover, in the absence of denuders to neutralize ammonia in the UDM, there could be neutralization of the acidic particles collected and possibly changes in their appearance when examined by AFM, resulting in lower particle numbers. Overall, the UDM results are difficult to interpret owing to uncertainties about the size range of the particles deposited on the detectors and about how the efficiency of deposition varies with particle size. Also unknown is the magnitude of error in the determination of deposition efficiency, which could be large.

The number concentrations obtained from the MOI-EAS detectors were lower than those derived from the comparison instrument, the SMPS, while those obtained from the UDM detectors were more similar to the corresponding SMPS measures (for some of the sampling periods). These results led the authors to conclude that the MOI-EAS underestimated the total number of ultrafine particles and would be likely to also underestimate the number of acidic ultrafine particles. This conclusion is plausible, but the reasons for the discrepancies were not investigated and are not understood.

The authors found no correlation between the number concentrations of acidic ultrafine particles (determined with the MOI-EAS) and the acid content of ultrafine particles (determined by measuring the pH of particles less than 100 nm in diameter, collected on the polycarbonate filter placed in parallel with the EAS after the last stage of the MOI). They comment that this finding indicates a complex relation between acid volume and number of acidic particles. This finding is intriguing and, if confirmed by further testing, suggests that conclusions about the association between health effects and exposure to acidic particles might be different if the number of acidic particles, rather than particle acidity, were evaluated.

The particle number counts determined continuously during 24-hour periods with the SMPS and CNC were in poor agreement at some times and good agreement at others. These results underscore the difficulty of comparing different instruments.

Although the iron nanofilm is promising for particle analysis, further work is needed to understand better how acidic and nonacidic particles of different sizes react with the nanofilm surface, and how the nanofilms perform in locations with higher levels of particles and gases (especially ozone, which is the gas most likely to react chemically with the iron nanofilm). The counting method presented here is labor-intensive and does not appear to be feasible for analyses of large sets of samples. State-of-the-art AFM technology may provide higher sample throughput, improved resolution of the reaction sites, and the ability to classify particles by size. However, in order to accomplish this, the relation between the size of the original particles and the size of the reaction sites would need to be established.

Further indoor tests would also be useful to evaluate how the iron nanofilm detector system performs under different conditions. The finding of higher ultrafine acidic particles inside the NIEM cafeteria than outside using the UDM is puzzling because acidic particles are generally neutralized by high levels of ammonia indoors. Although it

is conceivable that acidic particles were generated indoors, this finding remains to be explained.

Finally, the relatively long sampling period needed to obtain substantial material may limit the use of this method in epidemiologic studies when shorter temporal variations in particle levels are of interest. This is particularly important for ultrafine particles, which, as shown in the report, vary greatly in their level during the day. Additionally, particles less than 35 nm in size were not measurable with the available technology. These nanoparticles can constitute a large fraction of the total particle number concentration near roadways, and it would be useful to be able to detect and count them as well.

SUMMARY AND CONCLUSIONS

This study tested an iron nanofilm as a substrate in particle samplers for estimating the number of acidic particles in ambient air. Such a measure cannot be obtained presently with available instruments. Analysis of the exposed iron nanofilms by AFM yielded images of the nanofilm surface from which the number of acidic particles and the total number of particles were determined. The substrate was stable at average temperature (22°C) and high humidity, but some enlargement of the reaction sites occurred at the end of the 3-month storage period. Exposure to high humidity and high temperature (39°C) substantially compromised the integrity of the surface.

The field monitoring studies, conducted primarily in a rural location, showed that the iron nanofilm detector deployed in two sampling instruments, the MOI-EAS and the UDM, can be used to collect ultrafine particles. Agreement between the counts of acidic and total particles obtained with the two samplers over periods of 1 or 2 weeks was limited. In the absence of a comparison sampler that measures acidic particles, it is difficult to evaluate the accuracy of these two instruments for measuring acidic particles. In a comparison with the total ultrafine particle numbers measured with a commercially available continuous particle counter, the SMPS, the MOI-EAS counts were lower, but the UDM counts were similar. Despite this result, the UDM presently appears to have more inherent limitations than the MOI-EAS such as a less selective cut point, low deposition efficiency, and possible interference by ammonia.

Uncertainties regarding the rate of the reaction of acidic and nonacidic particles with the nanofilm, the relation between particle acidity and the shape of the reaction site, the collection efficiency of the samplers (especially the UDM), and the error in counting the reaction sites remain to be evaluated more extensively.

In summary, in the absence of other methods for measuring the number of acidic particles, iron nanofilms housed in an EAS may be used to approximate the ambient levels of acidic particles, although further improvements of the system are needed.

ACKNOWLEDGMENTS

The Health Review Committee thanks the ad hoc reviewers for their help in evaluating the scientific merit of the Investigators' Report. The Committee is also grateful to Debra Kaden for her oversight of the study, to Maria Costantini and Julianne Chen for their assistance in preparing its Critique, and to Genevieve MacLellan, Sally Edwards, Jenny Lamont, and Frederic Howe for their roles in publishing this Research Report.

REFERENCES

Amdur M. 1996. Animal toxicology. In: Particles in Our Air: Concentrations and Health Effects (Wilson R, Spengler JD, eds). Harvard University Press, Cambridge MA.

Amdur MO. 1989. Health effects of air pollutants: Sulfuric acid, the old and the new. Environ Health Perspect 81:109–113.

Amdur MO, Chen LC. 1989. Furnace-generated acid aerosols: Speciation and pulmonary effects. Environ Health Perspect 79:147–150.

Burtscher H. 2001. Literature Study on Tailpipe Particulate Emission Measurement for Diesel Engines. Report for the Particle Measurement Programme for BUWAL/GRPE. Diesel Particulate Filter Manufacturers Task Force (Arbeitskreis Partikel-Filter-Systemhersteller), Wien, Austria. Available at *www.akpf.org/pub/burtscher_bericht.pdf*.

Cohen BS, Li WL, Xiong JQ, Lippmann M. 2000. Detecting H^+ in ultrafine ambient aerosol using iron nano-film detectors and scanning probe microscopy. Appl Occup Environ Hyg 15:80–89.

Donaldson K, Li XY, MacNee W. 1998. Ultrafine (nanometre) particle mediated lung injury. J Aerosol Sci 29:553–560.

Environmental Protection Agency (US). 1997. National Ambient Air Quality Standards for Particulate Matter; Final Rule. 40 CFR, Part 50. Fed Regist 62:38651–38701.

Ferin J, Oberdörster G, Penney DP. 1992. Pulmonary retention of ultrafine and fine particles in rats. Am J Respir Cell Mol Biol 6:535–542.

Knutson EO. 1999. History of diffusion batteries in aerosol measurements. Aerosol Sci Technol 31:83-128

Kreyling WG, Scheuch G. 2000 Clearance of particles from the lung. In: Particle-Lung Interactions (Gehr P, Heyder J, eds). Marcel Dekker, New York NY.

Mauderly J, Neas L, Schlesinger R. 1998. PM monitoring needs related to health effects. In: Atmospheric Observations: Helping Build the Scientific Basis for Decisions Related to Airborne Particulate Matter (Albritton DL, Greenbaum DS, cochairs). Report of the PM Measurements Research Workshop, Chapel Hill NC, July 22 and 23, 1998. Aeronomy Laboratory of the National Oceanic and Atmospheric Administration, Boulder CO, and Health Effects Institute, Cambridge MA.

NARTSO (North American Research Strategy for Tropospheric Ozone). 2003. Particulate Matter Science for Policy Makers: A NARSTO Assessment, Part 2. Available from *www.cgenv.com/Narsto* (click on PM Science & Assessment).

Oberdörster G, Ferin J, Gelein R, Soderholm SC, Finkelstein J. 1992. Role of the alveolar macrophage in lung injury: Studies with ultrafine particles. Environ Health Perspect 97:193–199.

Schlesinger RB, Cassee F. 2003. Atmospheric secondary inorganic particulate matter: The toxicological perspective as a basis for health effects risk assessment. Inhalation Toxicol 15:197–235.

Schwela D, Morawska L, Kotzias D (eds). 2002. Guidelines for Concentration and Exposure-Response Measurements of Fine and Ultra Fine Particulate Matter for Use in Epidemiological Studies. European Commission, World Health Organization, Geneva, Switzerland.

Seaton A, McNee W, Donaldson K, Godden D. 1995. Particulate air pollution and acute health effects. Lancet 345:176-178.

Speizer FE. 1999. Acid Sulfate Aerosols and Health. In: Air Pollution and Health (Holgate ST, Samet JM, Koren HS, Maynard RL, eds). Academic Press, San Diego CA.

RELATED HEI PUBLICATIONS

Report Number	Title	Principal Investigator	Date*
Research Reports			
114	A Personal Particle Speciation Sampler	S Hering	2003
105	Pathogenomic Mechanisms for Particulate Matter Induction of Acute Lung Injury and Inflammation in Mice	GD Leikauf	2001
96	Acute Pulmonary Effects of Ultrafine Particles in Rats and Mice	G Oberdörster	2000
95	Association of Particulate Matter Components with Daily Mortality and Morbidity in Urban Populations	M Lippmann	2000
91	Mechanisms of Morbidity and Mortality from Exposure to Ambient Air Particles	JJ Godleski	2000
63	Development of Samplers for Measuring Human Exposures to Ozone		
	Active and Passive Ozone Samplers Based on a Reaction with a Binary Reagent	JD Hackney	1994
	A Passive Ozone Sampler Based on a Reaction with Nitrite	P Koutrakis	1994
	A Passive Ozone Sampler Based on a Reaction with Iodide	Y Yanagisawa	1994

** Reports published since 1990.*
Copies of these reports can be obtained from the Health Effects Institute and many are available at www.healtheffects.org.

HEALTH
EFFECTS
INSTITUTE

Charlestown Navy Yard
120 Second Avenue
Boston MA 02129-4533 USA
+1-617-886-9330
www.healtheffects.org

RESEARCH
REPORT

Number 121
September 2004